Top Curr Chem (2011) 300: 51–91
DOI: 10.1007/128_2010_99

Published online: 18 November 2010

Luminescence Amplification Strategies Integrated with Microparticle and Nanoparticle Platforms

Shengchao Zhu, Tobias Fischer, Wei Wan, Ana B. Descalzo, and Knut Rurack

Abstract The amplification of luminescence signals is often the key to sensitive and powerful detection protocols. Besides optimized fluorescent probes and labels, functionalized nano- and microparticles have received strongly increasing attention in this context during the past decade. This contribution introduces the main signalling concepts for particle-based amplification strategies and stresses, especially the important role that metal and semiconductor nanoparticles play in this field. Besides resonance energy transfer, metal-enhanced emission and the catalytic generation of luminescence, the impact of multi-chromophoric objects such as dye nanocrystals, dendrimers, conjugated polymers or mesoporous hybrid materials is assessed. The representative examples discussed cover a broad range of analytes from metal ions and small organic molecules to oligonucleotides and enzyme activity.

Keywords Luminescence, Multi-Chromophore systems, Nanoparticles, Resonance energy transfer, Signal amplification

Contents

S. Zhu, T. Fischer, W. Wan, and K. Rurack (✉)
Div I.5, BAM Bundesanstalt für Materialforschung und -prüfung, Richard-Willstätter-Str. 11, 12489, Berlin, Germany
e-mail: knut.rurack@bam.de

A.B. Descalzo
Div I.5, BAM Bundesanstalt für Materialforschung und -prüfung Richard-Willstätter-Str. 11, 12489, Berlin, Germany
Department of Organic Chemistry, Faculty of Chemistry, Complutense University of Madrid, Avda. Complutense s/n, 28040, Madrid, Spain

1 Introduction

Fluorescence spectroscopy is becoming an ever more valuable and popular tool in analytical and bioanalytical chemistry [1–3]. Its outstanding sensitivity and versatility as well as the fact that fluorescence inherently allows the exploitation of several different parameters all contribute to this ongoing success. Luminescence measurements provide information on the spectral, intensity, lifetime and polarization features of the fluorescing species. It is a non-destructive and non-invasive technique and when adequate fluorophores and equipment are employed it allows the measurement against a zero-background. Today, under the influence of modern analytical trends for miniaturized detection protocols, whether in combination with laboratory-based and sophisticated instrumentation for high-throughput analysis and screening in clinical diagnostics or pharmaceutical screening or for implementation into mobile, handheld devices in point-of-care-testing or homeland security applications, fluorescent probe or sensor systems have to become more and more powerful [4–7]. The detection volume or the active area or spot sampled in such miniaturized protocols is often much smaller than in conventional fluorescence applications so that the amount of luminescence generated by a single probe should be as high as possible. To go beyond the signal provided by a single fluorescent tag such as for instance a single Cy3 or FITC (fluorescein isothiocyanate) molecule, the development of fluorescence amplification strategies has received increasing attention. However, the amplification features of single fluorophore molecules are intrinsically limited. Even if the fluorophore's photoluminescence quantum yield (PLQY) amounts to 1, absorption of a single photon can only generate a single emitted photon. For fluorescent molecules as tags or labels, this limit cannot be surpassed. For fluorescent indicators or probes which indicate a certain target species by a specific change in fluorescence, strong signals are commonly only achieved when the PLQY of bound and unbound form differ as much as possible, i.e. when analyte-binding leads to a "switching on" of the fluorescence [8]. During

the last decade, several strategies have thus been proposed and realized to generate amplified fluorescence signals, many of them relying on nano- or microparticulate or -structured objects, surfaces of interfaces. These concepts range from the improvement of the signal-to-noise ratio over the suppression of unspecific signals and the collective response of more than one fluorophore unit on the binding event to the catalytic production of fluorophores and the direct amplification of photophysical processes. The present contribution will give an overview of the most prominent approaches and will highlight representative examples in this exciting area of research. (Bio)molecular amplification techniques that are very powerful yet only lead to an increased signal by the catalytic amplification of an analyte, which is then conventionally treated, like the polymerase chain reaction (PCR), will not be covered here [9]. In addition, the discussion of enzymatic approaches like the rolling-circle amplification (RCA) would also go beyond the scope of the present chapter [9]. For a more general introduction of signal amplification involving molecular indicators and detection schemes, the reader is referred to [10].

2 Resonance Energy Transfer

The first section deals with a concept that is in most cases not a true amplification strategy in the sense that one analyte as input generates an output from a larger number of fluorophores, but the advantageous features here are based on the uniqueness of the signalling system. The latter involves two chromophores and a distance-dependent process and enables one to separate the excitation wavelength significantly from the emission spectrum, creating a system with a very large pseudo-Stokes shift. The concept is called *resonance energy transfer* or RET and the mechanism can be rationalized as follows. After photo-excitation, the energy absorbed by a molecule (the RET donor, D_{RET}) can be transferred over a certain distance to another molecule (the RET acceptor, A_{RET}) through resonance energy transfer. In the ideal case, exclusive donor excitation thus leads to exclusive acceptor emission. The pronounced pseudo-Stokes shift which is especially important for experimental reasons such as the suppression of scattering and background signals is based on the fact that the experimentally relevant spectra are the absorption spectrum of the donor and the emission spectrum of the acceptor (1), while the mechanistically important spectra create the spectral overlap necessary for RET (Fig. 1) [11].

$$\Delta\tilde{\nu}_{\mathrm{Stokes}}^{\mathrm{pseudo}} = \tilde{\nu}_{\mathrm{abs}}(D_{\mathrm{RET}}) - \tilde{\nu}_{\mathrm{em}}(A_{\mathrm{RET}}) \approx \frac{1}{\lambda_{\mathrm{abs}}(D_{\mathrm{RET}})} - \frac{1}{\lambda_{\mathrm{em}}(A_{\mathrm{RET}})}. \qquad (1)$$

Resonance energy transfer can occur when the emission spectrum of the donor overlaps to a sufficient degree with the absorption spectrum of the acceptor (Fig. 1) and when the distance between the excited donor and the acceptor in the ground

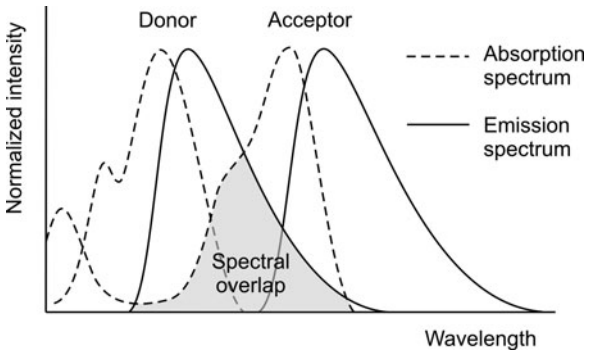

Fig. 1 Spectral characteristics of a RET system. The *highlighted area* corresponds to the mechanistically important overlap between emission spectrum of the donor and absorption spectrum of the acceptor. (Reprinted with permission from [11]. Copyright 2009 Springer)

state lies between 1–10 nm. In addition, it is important to keep in mind that the energy is transferred through a non-radiative process and that no fluorescence (of the donor) is involved. Nowadays, RET is a widely used and popular approach in several areas of analytical, life and materials sciences [12].

According to Förster's theory [13], the efficiency of the resonance energy transfer (E_{RET}) is inversely proportional to the sixth-power of the distance (r) between donor and acceptor (2). In (2), R_0 is the so-called Förster distance at which the transfer efficiency is 50%. Förster RET is therefore a very sensitive process and can transduce small conformational changes into large intensity modulations. R_0 is characteristic for a particular donor–acceptor pair and depends on the overlap integral J between D_{RET} emission and A_{RET} absorption, the PLQY of D_{RET} in its unperturbed state Φ_{D} and the mutual orientation of the two partners expressed as geometry factor κ^2 which equals 2/3 for random orientation of the partners (3). For a more detailed discussion of the mechanistics of RET, the reader is referred to the literature [12].

$$E_{\mathrm{RET}} = \frac{R_0^6}{R_0^6 + r^6}. \tag{2}$$

$$R_0{}^6 = 8.875 \times 10^{-5} \frac{\kappa^2 \Phi_{\mathrm{D}} J}{n^4} \quad \text{with} \quad J = \int F_{\mathrm{D}}(\lambda)\varepsilon_{\mathrm{A}}(\lambda)\lambda^4 \mathrm{d}\lambda. \tag{3}$$

Depending on the donor chosen, RET systems can be divided into fluorescence resonance energy transfer (FRET) systems for which the donor is a fluorescent molecule, nanocrystal or an object such as a dye-doped particle, bioluminescence resonance energy transfer (BRET) systems for which the donor is a bioluminescent molecule and chemiluminescence RET (CRET) systems, the chemical equivalent

of BRET, for which the donor is a chemiluminescent molecule, respectively [14].[1] Whereas FRET is unique in generating a fluorescence signal after photo-excitation of the donor, BRET and CRET measurements do not require an external light source and do not have to account for autofluorescence background signals because excitation occurs through a chemical reaction. Besides a zero-background, the main importance of BRET and CRET is that photo-damaging, especially of biological samples, is avoided. A comparison of FRET and BRET is summarized in Fig. 2 and the different advantages and disadvantages of the two strategies are discussed for instance in [15, 16].

RET in conjunction with nano- or microparticles can be principally divided into three different categories. First, dye-doped particles can be used as RET partner, usually as D_{RET}, and mostly a dye attached to the target analyte serves as the RET acceptor. The particles employed here are mainly polymer and silica particles and their size commonly lies between 20 nm and 2 μm. Moreover, this approach can be further divided into three strategies.

In the prevalent case, the particles are doped with a high amount of one particular dye (Fig. 3a). The main advantage is that such particles are generally highly fluorescent and, because of the large number of dyes incorporated, possess a statistical advantage of yielding a FRET signal once an adequately labelled target is bound (or a labelled probe is displaced). In addition, the incorporation of many dyes into a single particle and the equipment of the particle's surface with many binding sites allow the detection of many analytes on a single particle [17]. The second strategy uses the favourable features of RET as a tuning element, i.e. for the tuning of the pseudo-Stokes shift. Several dyes with matched absorption and emission bands are integrated into a single particle, creating one or more "tandem" FRET pairs within the particle (Fig. 3b). If properly tailored, such a cascade of dyes allows for efficient excitation energy transfer – efficiencies of >90% can be reached – and can yield pseudo-Stokes shifts of >200 nm [18], potentially shifting the emission bands far into the "biological window", i.e. into the spectral range of 650–900 nm [19]. However, up to now, such particles have been mainly used for bar-coding and multiplexing applications, allowing the tracking and identification of certain particles or analytes [20, 21]. A combination of such FRET-tandem dye-doped particles, for instance as D_{RET} partner in a classical FRET assay with a conventional dye as A_{RET}, has not yet been realized (for one of the few examples of

[1] The IUPAC-approved term for FRET is Förster RET [14]. 'Fluorescence resonance energy transfer' is commented on as the: *Term frequently and inappropriately applied to resonance energy transfer in the sense of Förster-resonance energy transfer (FRET), which does not involve the emission of radiation*. In contrast, the literature uses both terms Förster RET and fluorescence RET with the latter even dominating in the biochemical and bioanalytical communities. Despite the correct classification by the IUPAC, the scientist is in a dilemma when trying to distinguish between FRET, BRET and CRET, all Förster-type processes which differ only in the properties of the donor. Interestingly, BRET and CRET are not included in the IUPAC Photochemistry Commission's recommendations. In the present case, it seems more appropriate for us to use FRET for a RET involving a potentially fluorescent donor and BRET (CRET) for a RET involving a potentially bioluminescent (chemiluminescent) donor here.

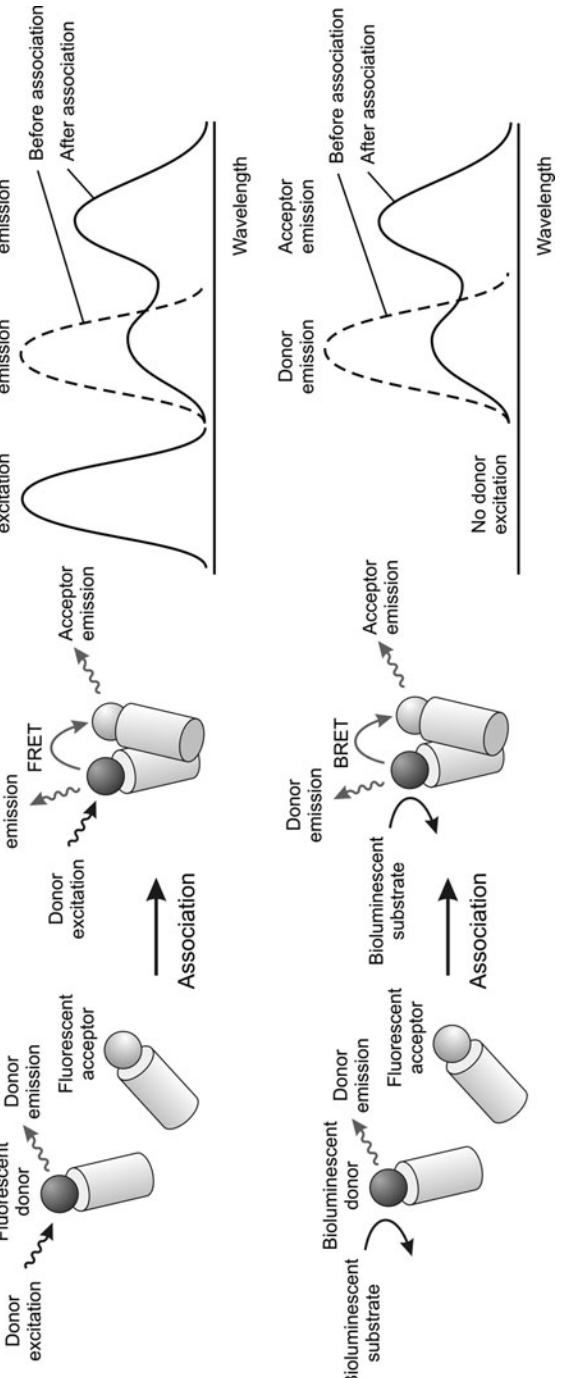

Fig. 2 Comparison of FRET (*top*) and BRET (*bottom*). (Reprinted with permission from [11]. Copyright 2009 Springer)

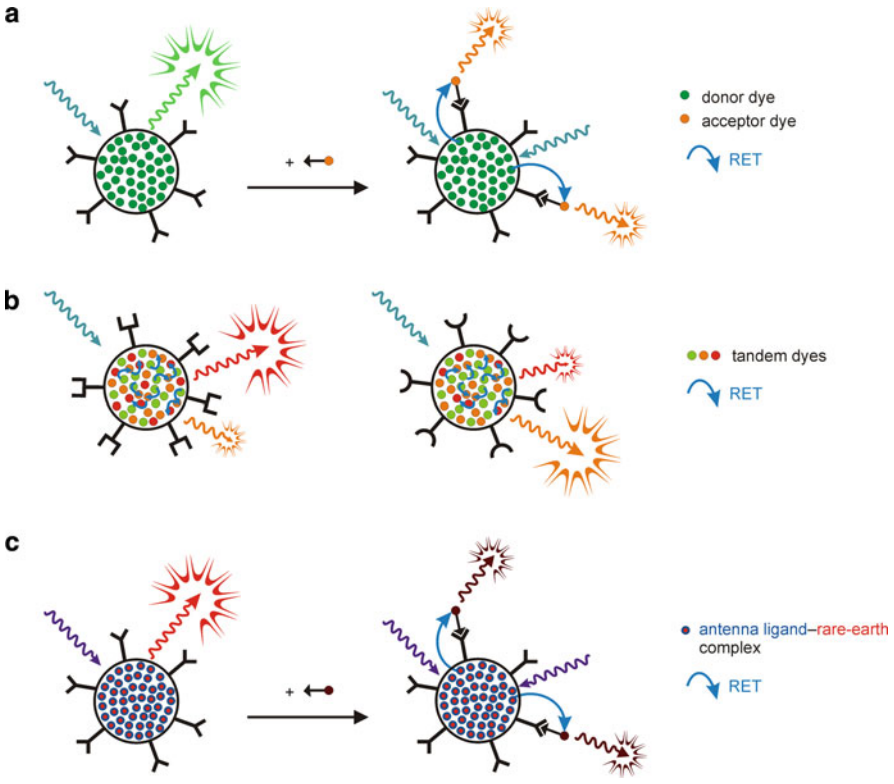

Fig. 3 Three different RET approaches involving polymer or silica particles as described in the text. (**a**) Particles doped with a large amount of a single dye for multiple FRET detection on a single particle; common case: excitation in the visible yields strong visible emission and *red-visible FRET signals*. (**b**) Particles with different receptors are doped with different ratios of FRET-tandem dyes yielding different emission colours for bar-coding or multiplexed detection; common case: excitation in the visible yields different emission colours in the *red-visible* and near infrared (NIR) range. (**c**) Particles doped with a rare earth–antenna ligand complex for multiple FRET detection on a single particle; common case: excitation in the UV yields strong red-visible emission through intra-complex energy transfer (not indicated in the sketch) and NIR FRET signals

FRET-tandems in a FRET assay, see Sect. 2.3 below). In a step further, the third strategy relies on rare earth emitters as D_{RET}. Because of the formally forbidden f–f transitions which are involved in rare earth luminescence and which possess only very low absorption coefficients, emitters such as Eu^{3+} or Tb^{3+} are usually complexed with an organic ligand which shows a sizeable absorption in the UV/vis region and is able to efficiently transfer its energy to the metal ion, i.e. to sensitize it. In the case of Eu^{3+}, for instance, such antenna ligands usually absorb in the 300–400 nm range while the strongest emission line of Eu^{3+} is found at 614 nm [22]. The ensemble antenna–rare earth cation thus intrinsically shows

the same features as the (multi-)tandem dye systems in the previous approach, i.e. pronounced pseudo-Stokes shifts, and can be doped into particles used as D_{RET} in a classical FRET approach (Fig. 3c). However, since the decay of the rare earth luminescence is quite slow, on the micro- to millisecond timescale again due to the f–f transitions involved, employment of particles doped with rare earth antenna chelates makes time-gated detection possible. Observation of the luminescence signal at a strongly pseudo-Stokes shifted wavelength with a time delay of several microseconds suppresses any background or autofluorescence signals most efficiently. Ultrasensitive assays can thus emerge [23].

The second category of particle-based RET systems utilizes inorganic particles such as gold nanoparticles (AuNPs), quantum dots (or semiconductor nanocrystals, QDs) or so-called up-conversion phosphor nanoparticles (or nanophosphors, UCPs) as one (or both) of the RET partners. These inorganic species are employed because of their unique and partly very favourable optical properties. AuNPs mainly function as efficient RET quenchers, QDs are basically employed as D_{RET} with high molar absorption coefficients and possible broad-band excitation and UCPs are particularly interesting because they can be excited with near infrared (NIR) light, show high PLQYs and very good chemical and photostability. Examples of these systems will be discussed in detail in the following sections.

The third category comprises metal NPs able to host surface plasmons that absorb in the visible spectral range and can therefore modulate intrinsic photophysical properties of organic dye molecules (and semiconductor nanocrystals), thus generating amplified signals. This last approach is discussed below in Sect. 5.2.3 together with other features of surface plasmon resonance (SPR) and metal-enhanced fluorescence (MEF). Due to this versatility in system design and the partly strong signal enhancement that can be achieved, micro- and nanoparticles are very popular building blocks in resonance energy transfer systems with improved performance in chemical and biochemical analytical applications.

2.1 Gold Nanoparticles

Gold nanoparticles (AuNPs) have several distinct advantages which qualify them as suitable RET partners in enhanced signalling applications. With respect to experimental issues, AuNPs are chemically and photochemically stable, do not show fluctuating signals and possess a very versatile functionalization chemistry. In addition, their synthesis in sizes that are still appropriate for RET applications, i.e. usually ca. 1–100 nm, is straightforward. Moreover, especially in this size range, they show intense (and size-dependent) SPR bands in the experimentally important visible wavelength range [24, 25].

AuNPs are almost exclusively used as potent quenchers in traditional RET applications. This is due to the fact that AuNPs of lower nanometric size efficiently quench the fluorescence of dyes because of a strong reduction of the radiative rate constant of the dye in close vicinity of the particle. In addition, the non-radiative

rate constant is increased when the fluorophore approaches the gold surface, however, with a much less dramatic effect. If the overall reduction in PLQY is considered, recent studies by Klar and Parak have shown that quenching is very efficient for AuNP–dye distances <4 nm but sizeable quenching is still found up to ca. 12 nm [26]. RET assays relying on AuNP are thus commonly designed in such a way that a non-luminescent FRET pair is formed between a potentially (highly) fluorescent D_{RET} dye and an AuNP as A_{RET} in the absence of the analyte. Binding of the target then liberates D_{RET}, reviving (strong) donor emission. For instance, an AuNP-based sensor for the detection of Hg^{2+} ions in aqueous solution has thus been developed, showing a strong modulation of the photoluminescence in the presence of the heavy metal ion. The assay is very potent and results in a 400-fold fluorescence enhancement in aqueous solution with analysis times of less than 10 min [27]. In a similar fashion, a FRET assay using a perylene bisimide (PBI) chromophore and AuNPs has been designed for Cu^{2+} [28]. The PBI chromophore carries two remote pyridine groups which coordinate to two AuNPs, invoking efficient quenching. Cu^{2+} complexation to the pyridine moieties unlocks the dye from the quenchers and revives emission. Because AuNP-mediated quenching is very efficient and considerably far reaching, the pyridine groups can be placed sufficiently far from the chromophore so that binding of the paramagnetic target does not result in fluorescence quenching in the liberated dye–Cu^{2+} complex. These examples show that FRET signalling can also elegantly accomplish the turn-on detection of notoriously quenching analytes such as Hg^{2+} and Cu^{2+}.

Besides metal ions, AuNPs are also popular quenchers in small-molecule and biomolecule RET assays. For example, a homogeneous sandwich immunoassay utilizing AuNPs as quenching acceptors has been reported for the detection of the protein cardiac troponin T (cTnT). As depicted in Fig. 4a, one of the antibodies (M11.7) is coupled to AuNPs and the other antibody (M7) is labelled with fluorescent Cy3B dyes [29]. In the absence of cTnT, the dyes emit their characteristic fluorescence. In the presence of cTnT, however, the two antibodies conjugate in sandwich arrangement and the fluorescence of the dyes is quenched by the AuNPs. Upon addition of analytes, the number of sandwich conjugates first increases, reaches a maximum, and then decreases again (Fig. 4a, bottom). The latter effect is measured above a certain threshold concentration of cTnT, when two antibodies do not bind in a sandwich fashion but individually to two analytes. Consequently, the fluorescence intensity decreases first, reaches a minimum, and increases again. For unambiguous quantification, careful system adjustment is thus necessary.

A popular field for AuNP-based FRET systems is DNA analysis. In an exemplary assay to monitor DNA cleavage, AuNPs have been functionalized with a Cy3-labelled oligonucleotide probe through a thiol–gold bond. Since the single-stranded probe wraps around the NP, the dye is close to the AuNP's surface and its fluorescence is strongly quenched. In the presence of the complementary target oligonucleotide, a double strand is formed, and the probe is moved away from the surface yet, in this design, is still within the quenching distance of the AuNP. Only after cleavage of the double strand from the particle by a single-strand specific nuclease is the Cy3 fluorescence revived. This assay is much faster and shows a

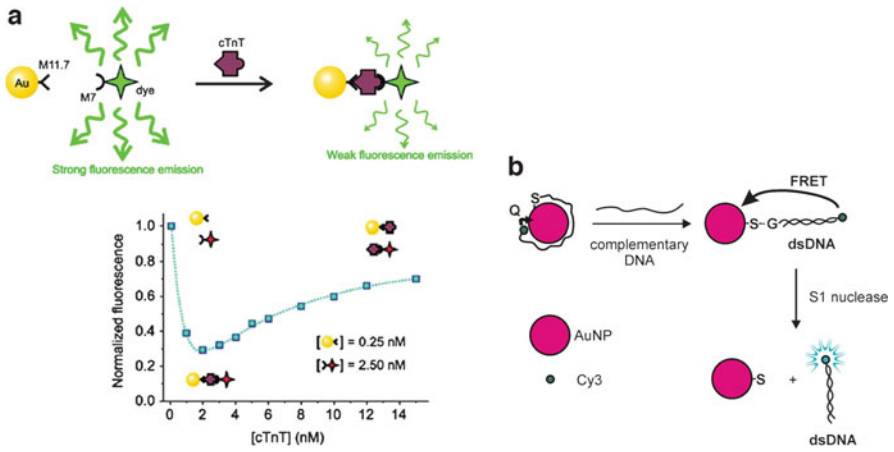

Fig. 4 (**a**) Schematic illustration of sandwich immunoassay for cTnT (*top*) and fluorescence intensity reading versus cTnT concentration (*bottom*). (**b**) Schematic illustration of the monitoring of DNA cleavage from AuNPs by a single-strand nuclease. (Reprinted and adapted with permission from [29, 30]. Copyright 2009, 2006 American Chemical Society)

sensitivity increase by several orders of magnitude compared to the traditional HPLC methods in assessing DNA cleavage (Fig. 4b) [30].

2.2 Quantum Dots

Quantum dots (QDs) or semiconductor nanocrystals have recently received strong attention in analytical chemistry because of their narrow emission bands, tuneable size-dependent emission spectra, spanning from the UV to the NIR, high PLQYs and high photostability [31, 32], including applications from fibre-optic sensing to multiplexed detection [33, 34]. Due to their broad excitation and narrow emission bands, QDs are ideal donors in FRET systems [35, 36]. Until recently, applications of QD-based RET probes have mainly used one of the following two approaches: (1) a QD as D_{RET} and a dye as A_{RET}, e.g. attached to a protein or DNA strand and (2) a QD as D_{RET} and a gold nanoparticle as A_{RET} quencher [37]. The scenario employing a QD as D_{RET} and a fluorescent protein as A_{RET} is less frequent [38] as is the case that uses a QD as D_{RET} and a conjugated polymer (CP) as A_{RET} (see below). Furthermore, approaches with two differently coloured QDs do not play a significant role yet in analytical chemistry [39], but are more important in the context of luminescent thin films and layer-by-layer architectures for various materials chemistry applications [40].

An elegant establishment of case (1) has been realized in conjunction with an aptamer-based recognition motif [41]. Here, a core-shell-type CdSe/ZnS QD is used as D_{RET} and an Atto 590 dye as A_{RET}, yielding enhanced red emission upon

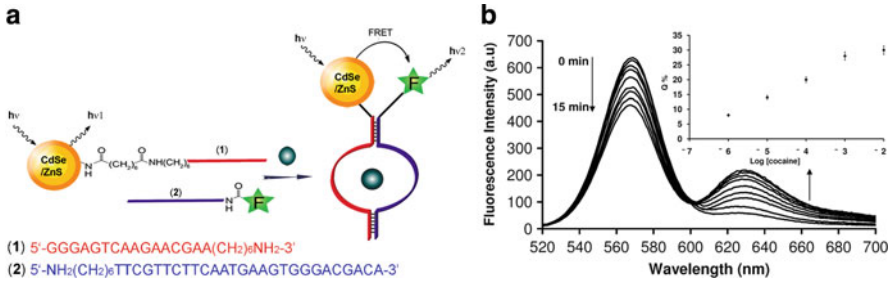

Fig. 5 (**a**) QD-based sensing of cocaine by the formation of a cocaine–aptamer supramolecular structure that triggers FRET. (**b**) Time-dependent luminescence spectra of the system in the presence of cocaine. The *inset* shows a calibration curve for variable concentrations of cocaine and a fixed observation time of 15 min. (Reprinted with permission from [41]. Copyright 2009 Royal Society of Chemistry)

Fig. 6 Schematic illustration of a QD-based FRET competition assay for TNT detection. (Reprinted with permission from [42]. Copyright 2005 American Chemical Society)

binding in the presence of the analyte cocaine (Fig. 5). Another example utilizing a FRET-quencher design has been realized for the detection of 2,4,6-trinitrotoluene (TNT). The system consists of a QD (CdSe/ZnS core-shell) and a quencher dye (Black Hole Quencher-10) as the FRET pair (Fig. 6). The QD is coupled with an anti-TNT antibody, and the quencher conjugated with the TNT analogue. The competition assay induces the inhibition of the FRET quenching process and thus enhances the fluorescence signal upon displacement of the quenching conjugate in the presence of a TNT molecule that can successfully compete for the binding site [42].

A representative example for case (2) introduced above consists of positively charged CdTe QDs capped with cysteamine (CA-CdTe QDs) and negatively charged AuNPs capped with 11-mercaptoundecanoic acid (MUA-AuNP) as FRET pair based on electrostatic attraction. In the absence of the target, the QD luminescence is effectively quenched in the FRET ensemble. The presence of Pb^{2+} then leads to a displacement of the CA-CdTe QDs and Pb^{2+}-mediated aggregation of the MUA-AuNPs, thus inhibiting the FRET process. An interesting aspect of this approach is that indication of the analyte is transduced by an enhancement of the

QD luminescence and a shift in the plasmon absorption band because of AuNP aggregation [43]. An example for the detection of a small-molecule analyte has been realized in a similar fashion as a nanobiosensor for glucose in serum. The QDs are conjugated with concanavalin A (ConA) and the AuNPs are coupled with thiolated β-cyclodextrins (β-SH-CDs), respectively. In the presence of glucose, the AuNP–β-SH-CD segment is displaced by the sugar which competes with β-CD for the binding sites of ConA, resulting in luminescence recovery of the quenched QDs [44].

Electrostatic complex formation between a fluorescent CP and CdTe QDs is another promising way to generate strong FRET signals. The example shown in Fig. 7 has been developed for the detection of target DNA hybridization. In the complex, the cationic polymer poly[9,9-bis(3′-((*N*,*N*-dimethyl)-*N*-ethylammonium)propyl)-2,7-fluorene-*alt*-1,4-phenylene]dibromide (PDFD) is used for both light-harvesting and assembling of the negatively charged QDs and DNA molecules [45]. This is one of the few cases where QDs act at the same time as $A_{\mathrm{RET}(1)}$ and $D_{\mathrm{RET}(2)}$. (For selected examples of CP-based FRET assays, see Sect. 3.1.)

Owing to the broad absorption/excitation spectra of QDs, they can be excited by nearly all the bioluminescent proteins available and are thus suitable A_{RET} in BRET systems, taking advantage of the virtual absence of background fluorescence. For instance, a QD-based BRET assay has been developed by coupling carboxylate-functionalized QDs to a mutant of the bioluminescent protein *Renilla reniformis* luciferase (Fig. 8). Once stimulated, the ensemble emits long-wavelength bioluminescence light in cells and deep tissues. This advantage distinguishes bioluminescent QD probes as a very promising approach toward sensitive in vivo imaging, in vitro assays and multiplexing analysis [46].

Besides BRET, there is another less frequent RET method called chemiluminescence resonance energy transfer (CRET). CRET is closely related to BRET, utilizing a chemiluminescent (CL) instead of a bioluminescent D_{RET}, i.e. CRET commonly relies on the oxidation of a potentially luminescent substrate. Like BRET, CRET can dispense with an excitation source and thus shows excellent background suppression. A model CRET assay has been realized with bovine serum albumin- (BSA) coupled CdTe QDs and anti-BSA antibodies conjugated to horseradish peroxidise (HRP). Together with luminol as the substrate, HRP

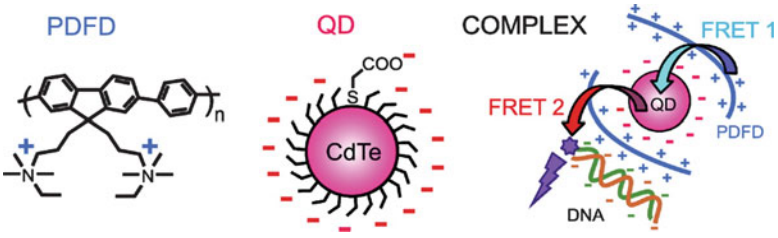

Fig. 7 Chemical structure of PDFD, schematics of a thioglycolic acid (TGA)-capped CdTe QD and of the PDFD/QD/dye-labelled DNA complex for detecting DNA hybridization. (Reprinted with permission from [45]. Copyright 2009 American Chemical Society)

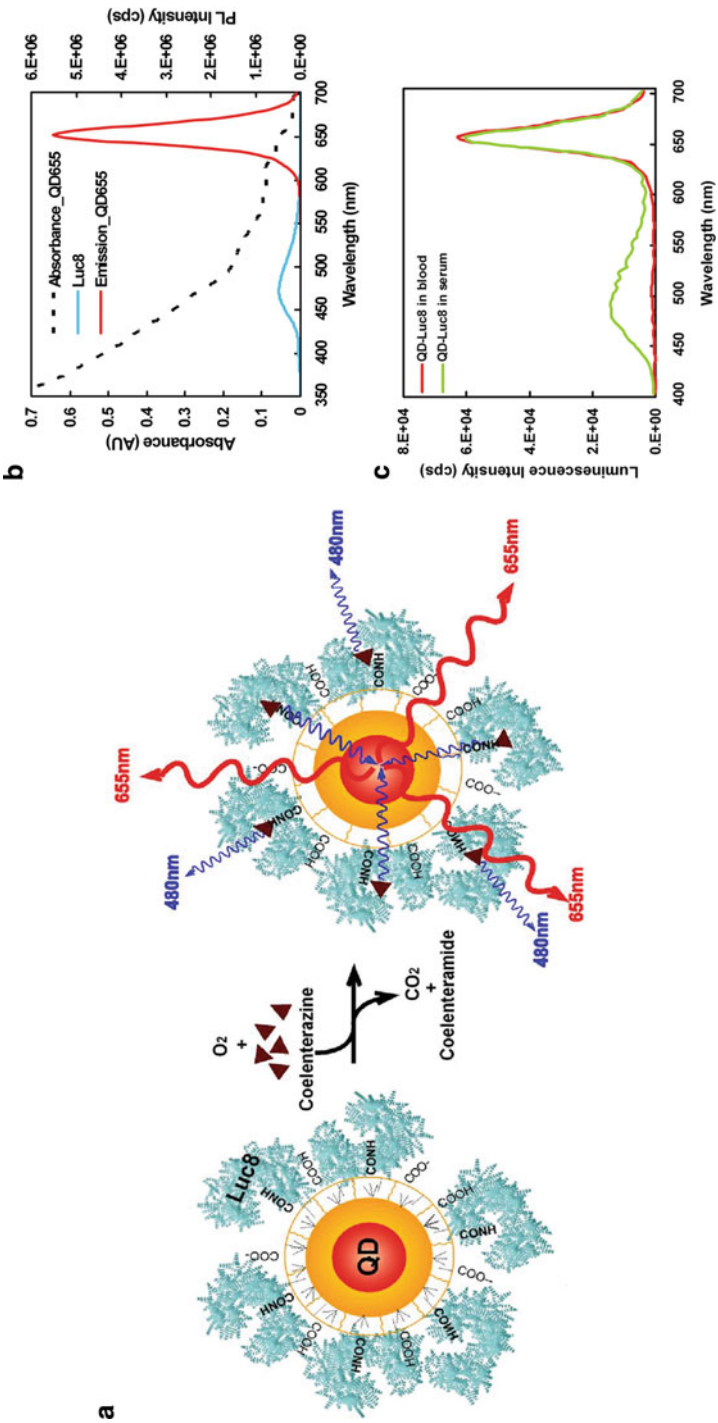

Fig. 8 (**a**) Schematic illustration of the QD-based BRET system and (**b**) spectral manifestation of the assay. (**c**) Two assays performed under identical conditions in mouse serum (*green*) and mouse whole blood (*red*). (Reprinted with permission from [46]. Copyright 2006 Macmillan Publishers Ltd)

constitutes a classical CL system and continuously catalyzes the production of chemiluminescence with, for instance (and like in this case), hydrogen peroxide as the oxidant. Once the QD-labelled BSA binds to the antibody, CL production occurs close enough in space to trigger red-shifted CRET emission from the QD as A_{RET} [47]. This method has significant potential for applications in immunoassays of various types. Recently, Zhao et al. also showed that CRET systems can be used in a rather unspecific manner as a very sensitive detection scheme in microfluidic separation techniques [48].

2.3 Up-Conversion Nanoparticles

As mentioned above, recent research has seen the introduction of another alternative RET partner, the so-called up-conversion (nano)particles (UCPs). UCPs are excited in the NIR region and emit in the visible range through the sequential absorption of two or more low-energy photons [49]. UCPs basically consist of a host material doped with lanthanide ions. Although they have only a short history in (bio)chemical signalling, they hold great potential for analytical applications because of their favourable characteristics such as high PLQYs, tuneable optical properties, high chemical stability and low toxicity [50, 51].

Until today, up-conversion particles have mainly been used as donors in RET assays. For instance, they have been employed in combination with AuNPs as A_{RET} for the detection of trace amounts of avidin [52]. In the sandwich-type assay, emission of biotinylated UCPs is recorded prior to conjugation of biotinylated AuNPs in the presence of avidin. The AuNP-mediated quenching of the UCP luminescence then shows a linear relationship with avidin concentration. An attractive homogeneous assay format based on up-conversion RET has been established in a competitive immunoassay for estradiol (E2). Whereas the UCPs coated with an anti-E2 antibody serve as D_{RET}, E2-conjugated Oyster-556 dyes are employed as A_{RET} (Fig. 9) [53]. Since here D_{RET} can be excited well in the NIR, autofluorescence and scattered light are successfully eliminated and do not perturb the A_{RET} signals in the visible range. Furthermore, the introduction of tandem dyes in conjunction with UCPs can dramatically enhance the acceptor emission [54].

3 Nanoscopic Objects with Inherent Signal Amplification

Whereas the implementation of specific photophysical processes to generate well-separated and strongly distance-dependent signals has been the focus of the previous section, the examples presented in the following will show how the encapsulation of chromophores in nanoscopic systems can lead to amplified signals when compared with the respective molecular systems. Signal enhancement can be a consequence of different factors. For example, in a similar manner as briefly

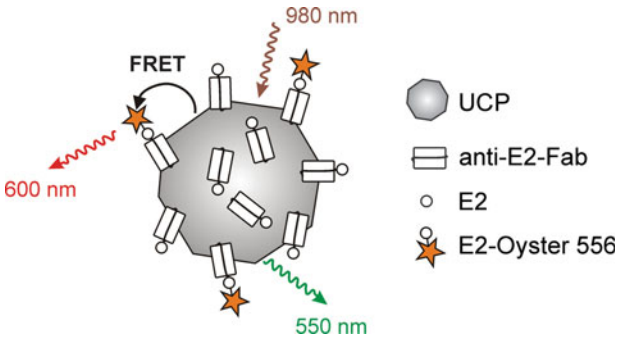

Fig. 9 Schematic illustration of UCP-based homogeneous FRET immunoassay for E2. (Adapted with permission from [53]. Copyright 2006 American Chemical Society)

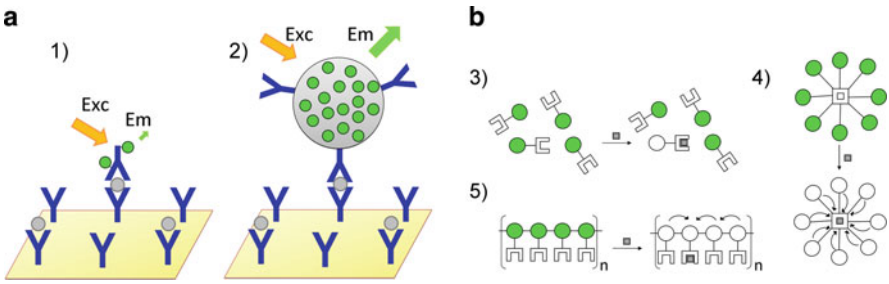

Fig. 10 (**a**) Representative scheme for the signal amplification concept by increasing the number of fluorophores per binding site in an antigen–antibody sandwich assay. Binding of a labelled antibody to the target yields an only moderate fluorescence signal because the antibody can be labelled with only a few fluorophores at maximum (1). Use of an antibody which is labelled with a nanoscopic object that contains a large number of fluorophores dramatically enhances the signal (2). (**b**) Effect of analyte coordination in (3) a traditional molecular indicator, (4) a fluorescent dendrimer and (5) receptors wired in series in a conjugated polymer. The *curved arrows* indicate the active processes, e.g. quenching

discussed in Sect. 2 (cf. Fig. 3a), the *increase of the number of luminophores per binding site* (i.e. the L/B ratio) can lead to an enhanced luminescence signal when *dendrimers*, *fluorescent nanocrystals* or *liposomes* are used as labels in binding assays, because every binding event is signalled by several tens, hundreds or thousands of fluorophores (Fig. 10). Collective *energy migration* or *energy transfer* processes, the latter closely related to the processes presented above, can also entail signal amplification, because, in contrast to conventional fluorescent indicator molecules, for which the recognition of the target by the receptor unit only affects the fluorescence properties of the single, covalently coupled fluorophore residue, in multi-fluorophore/multi- or single-binding site systems, more than one fluorophore unit can experience a modulation through a single binding event in its immediate neighbourhood. The underlying basis here is inter-fluorophore communication

which can occur in systems such as *fluorescently doped dendrimers* when the local concentration of fluorophores is comparatively high. Alternatively, analyte binding at a single receptor unit can influence multiple fluorescent repeat units of a *CP* because of the electronically delocalized structure of CPs which facilitates energy migration over large distances to the analyte–receptor complex as a "sink". The net effect in all of these cases is the transduction of a single binding event by an amplified response of several fluorophores.

Representative examples of signal amplification in CPs, fluorescent dendrimers, encapsulated dye microcrystals as well as dye-loaded liposomes and mesoporous silica hybrids will be discussed below. For examples involving luminescently doped silica or polymer particles, which are very similar in nature, the reader is referred to [55].

3.1 Conjugated Polymers

The dominant attribute that has driven interest in fluorescent CP sensory materials is their ability to produce signal gain in response to interaction with analytes. The increased sensitivity (amplification) is derived from the ability of the CP's delocalized electronic structure (i.e. energy bands) to facilitate efficient energy migration over large distances. To rationalize how energy migration can amplify fluorescence-based sensory events, consider a CP with a receptor attached to every repeating unit. If energy migration is rapid with respect to the fluorescence lifetime, then the excited state can sample every receptor in the polymer, thereby allowing the occupation of a single binding site to change dramatically the entire emission of the system (Fig. 10b).

A first proof-of-principle for the signal amplification phenomenon in CPs has been reported by Zhou and Swager in 1995. By using poly(propylene ethynylene) as CP with 34-crown-10 groups attached to the CP as receptors for the recognition of the well-known quencher paraquat (PQ^{2+}), the authors could observe how PQ^{2+} binding produced a trapping site for excitons, which were effectively deactivated by electron transfer [56]. CPs have been employed in different formats like in homogeneous solution, as thin films or as molecularly imprinted polymers. A comprehensive overview of further examples and mechanistic descriptions of CP-based signalling systems can be found in [57].

CPs can also be prepared in nanoparticulate form [58–62]. The interesting aspect of such a formulation is that first reports have appeared which discuss how CP NPs can yield even stronger signal amplification. For example, silica NPs covered with layers of CPs have been employed for the detection of nitroaromatic quenchers with sensitivity enhancement factors of up to 200 with respect to the corresponding neat polymers in solution. Interestingly, in all cases, the microspheres coated with two layer pairs of CPs show larger Stern–Volmer quenching values than those coated with only one layer pair, which was ascribed to an energy migration effect [63].

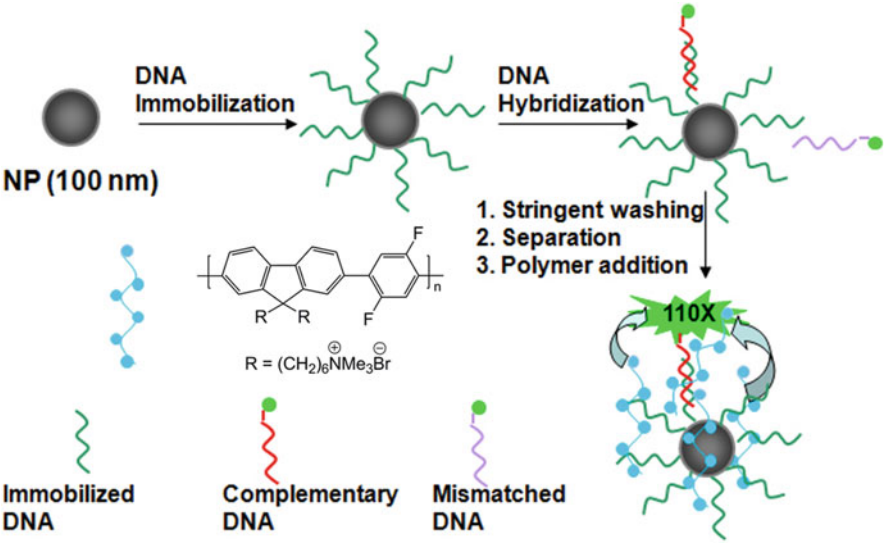

Fig. 11 Signal amplification with CPs via FRET in a DNA hybridization assay on silica NPs. First, the silica NPs are functionalized with the capture DNA. After DNA hybridization with a complementary dye-labelled DNA strand and subsequent washing and separation, CP is added, resulting in a 110-fold fluorescence increase. (Reprinted with permission from [67]. Copyright 2007 Royal Society of Chemistry)

CPs have also been successfully employed as energy harvesting systems in FRET based assays [64, 65] (for an introduction to resonance energy transfer, see Sect. 2). For instance, Liu et al. have used this property for amplifying fluorescence signals in silica NP-based FRET immunoassays [66] and DNA hybridization assays [67, 68], in a way resembling the enhanced excitation intensities at metal surfaces discussed in Sect. 5.1. The amplified emission by excitation of the CP relative to direct excitation of the dye label originates from the electron-delocalized backbone of the CP that allows rapid intrachain and interchain exciton migration via RET (Fig. 11) [67]. In a later work, the same authors have reported the surface functionalization of polyhedral oligomeric silsesquioxane (POSS) nanoparticles of 3.6 nm diameter with cationic oligofluorene for fluorescence amplification in cellular imaging. The cationic oligofluorene substituted POSS (OFP) possesses outstanding light harvesting properties for efficient RET. As a result, the fluorescence of intercalated ethidium bromide is amplified 52-fold upon excitation of OFP in buffer [69].

3.2 Dendrimers

A unique concept that can be employed when aiming to install energy funnelling processes and at the same time aspiring to increase the L/B ratio relies on *dendrimers*. Dendrimers are highly branched, tree-like polymers that possess a precise size and

shape and defined surface groups. They are multifunctional macromolecules which can bear multiple dyes and biomolecules. Fluorescent dendrimers have been used for instance for signal amplification in DNA assays using flow cytometry techniques. With the dendrimer assay, the minimum detectable amount of analyte DNA has been lowered from hundreds to tens of attomoles [70]. Dendrimers labelled with different families of organic dyes can also serve as strongly fluorescent probes for the detection of biomacromolecules [71].

Regarding *energy migration* in nanoscopic systems, dendrimers containing photoactive components can exhibit particularly interesting properties since cooperation among the photoactive units can allow the dendrimer to perform specific functions, e.g. light harvesting through antenna effects. Properly designed dendritic materials can show efficient migration of energy from the dendrons or peripheral groups to the more conjugated units or core, leading to dramatically enhanced fluorescence intensity changes (Fig. 10b). One of the first works realizing the application of dendrimers in optical sensing and signal amplification has been conducted by Vögtle, Balzani et al. [72]. They have used a fourth generation (4D) poly(propylene amine) dendrimer with 32 dansyl units at the periphery and containing 30 aliphatic amine units in the core for the detection of Co^{2+}. The fluorescence of all dansyl units is quenched when a single Co^{2+} ion coordinates to the aliphatic amine units. In a further work, another sensory dendrimer and a mono-dansylated reference compound have been investigated for comparison. Addition of Ni^{2+} or Co^{2+} to a basic solution of the mono-dansyl compound did not cause any effect in the absorption or emission properties of the molecule. However, in the case of the dendrimer – now a polylysin dendrimer branched at the 1,3,5-positions with eight fluorescent dansyl units in the periphery and six aliphatic amide units in the interior of each branch – a strong quenching of the dansyl emission at 514 nm has been observed [73]. At low metal ion concentration, each metal quenches ca. nine dansyl units. Interestingly, the authors have also observed an influence of the dendrimer size on the response, i.e. quenching of the signal is amplified with increasing dendrimer generation, *n* [74].

Optically active dendrimers have also been described for fluorescence detection of chiral compounds, like those based on chiral 1,1′-bi-2-naphthol (BINOL) [75]. The light harvesting antennas of the dendrimer funnel energy to the central BINOL unit, whose hydroxyl groups lead to fluorescence quenching upon interaction with a chiral amino alcohol. This mechanism renders the dendrimers' fluorescence responses much more sensitive than those of the corresponding small-molecule sensors. The enantioselective fluorescence recognition of mandelic acid, a chiral α-hydroxycarboxylic acid, has also been realized in such a way [76]. This last example is particularly interesting because, in contrast to the majority of systems, the light-harvesting effect in this case entails fluorescence enhancement instead of quenching.

Mechanistically, exciton migration phenomena seem to be responsible for the enhanced fluorescence quenching in dendrimers. Investigations of Guo et al. have shown that the quenching constant for a fluorescent dendrimer in the presence of TNT increases with the dendrimer generation number. They have also shown that

excitons can migrate over the dendrimer surface to the quenching site, the ability for exciton migration being the main contributor to the observed dynamic fluorescence quenching [77].

3.3 *Encapsulated Dye Nanocrystals*

Leaving specifically tailored photophysical processes aside, the simplest way to increase the number of emitters per binding site is perhaps to use *fluorescent nanocrystals* instead of a molecular label. Renneberg et al. have introduced this concept in 2002 and encapsulated crystalline fluorescein diacetate (FDA) with an average size of 500 nm in ultrathin polyelectrolyte layers of poly(allylamine hydrochloride) and poly(sodium 4-styrene sulphonate) via layer-by-layer (LbL) techniques [78]. The polyelectrolyte coating is subsequently used as an interface for the attachment of antibodies through adsorption. The L/B ratio, ranging from 5×10^4 to 2×10^5, yields amplification rates of 70- to 2,000-fold for the nanocrystal label-based assay compared with the corresponding immunoassay performed with conventional, directly fluorophore-labelled antibodies. After the immunological reaction, the nanocrystals are dissolved by a release reagent and the dissolved molecules are released into the surrounding medium (Fig. 12). In subsequent works, the authors have optimized the performance of the assay by simplifying the preparation of the fluorescent conjugates. Assessing the analytical performance of the nanocrystal-based label system with a model sandwich

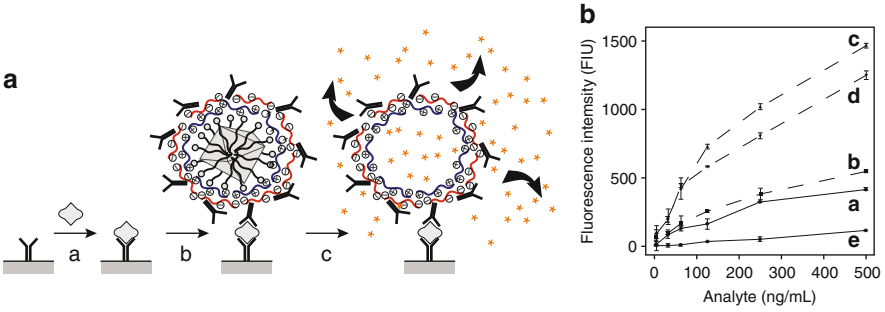

Fig. 12 (**a**) Principle of a sandwich immunoassay using FDA particulate labels. The analyte is first immobilized by the capture antibody pre-adsorbed on the solid phase (a) and then exposed to antibody-coated microparticle labels (b). Every microparticle contains ~10^8 FDA molecules. High signal amplification is achieved after dissolution, release and conversion of the precursor FDA into fluorescein molecules by the addition of DMSO and NaOH (c). (**b**) Calibration curves of IgG-FDA microcrystal labels with increasing surface coverage of detector antibody (a–d) compared with direct FITC-labelled detector antibody (e). The fluorescence signals increase with increasing IgG concentration. FDA microcrystals with a high IgG surface coverage (c,d) perform better than those with lower surface coverage (a,b). (Reprinted with permission from [78]. Copyright 2002 American Chemical Society)

immunoassay for the detection of mouse IgG, the authors could lower the LOD by a factor of 5–28 and increase the sensitivity 400- to 2,700-fold compared with conventional fluorescein isothiocyanate (FITC) conjugates [79]. The method has also been employed for avidin–biotin protocols [80] and for the quantitative detection of a PCR product [81].

3.4 Functionalized Liposomes

In a similar sense as discussed in the previous section, functionalized liposomes can be utilized as labels showing increased L/B ratios. Liposomes are synthetic spherical structures composed of one or more phospholipid bilayers in which soluble markers of interest can be encapsulated. This is commonly accomplished in two different ways. In the first approach, the dyes are embedded in the aqueous inner volume. For instance, Truneh et al. have included several hundreds of carboxyfluorescein and sulforhodamine fluorophores in a single liposome, which is then used to label an antibody [82]. Alternatively, if the dyes possess a more hydrophobic character like, e.g. perylene dyes, they can also be incorporated into the bilayer membrane [83]. A 500-fold signal enhancement with dye-encapsulating liposomes over single fluorophore labels has been demonstrated by Edwards and Baeumner for the detection of specific DNA oligonucleotide sequences [84].

Liposomes can be detected either directly or through release of their cargo, e.g. after detergent-induced degradation once the analyte has been traced. The signal is then generated by the fluorophores which are liberated into the solution [85]. Although this approach is attractive, the preparation of microcapsules with liposomes is rather elaborate and the stability of the systems is often critical. Analogues of liposomes are nanosome systems which are prepared with amphiphilic block-copolymers. These vesicles can also encapsulate water-soluble fluorophores in the inner aqueous phase. Cross-linking of the vesicle membrane allows tuning of permeability, enhanced stability under physiological conditions and preservation of size and structure [86].

3.5 Gated and Dye-Loaded Mesoporous Particles

The liberation of a large number of indicator dyes by a distinctly smaller number of analytes can also be accomplished with another type of nanoscopic amplification system that utilizes mesoporous particles and various gating chemistries for locking and unlocking of the pore openings. The materials commonly employed here are organic-inorganic hybrid mesoporous silica nanoparticles. The basic concept includes the simple steric loading of a large number of dye molecules into the pores of the nanoparticle and the closing of the pore openings by attachment of a comparatively small number of sufficiently large molecules on the particle surface

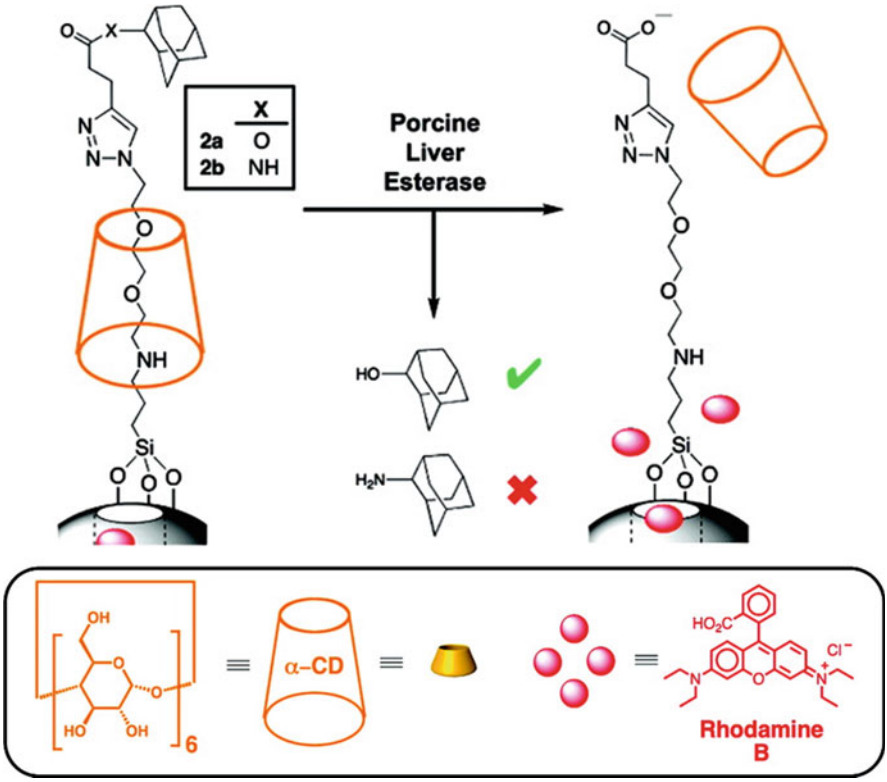

Fig. 13 Enzyme-mediated opening and dye release mechanism with selectivity for ester bond cleavage. (Reprinted and adapted with permission from [88]. Copyright 2008 American Chemical Society)

that block the pores. In contrast to drug delivery applications for which various gating mechanisms including redox and photo-switchable processes have been designed [87], the few systems developed for luminescence sensing rely on the oldest chemical technique for pore opening, a chemical reaction in the presence of the analyte that leads to the cleavage of the stopper. An inherent feature of this gating strategy is its nature as a truly amplifying process.

Although not yet established for analyte sensing, the enzyme-mediated release of dyes from porous silica particles as it has been recently developed to model nanocontainer-based, site-selective drug delivery can serve well as a representative example to illustrate the concept (Fig. 13) [88]. Rhodamine B which has been used as the model indicator dye is loaded into the mesopores of the silica material and entrapped by capping with a rotaxane, consisting of an ethylene glycol thread encircled by an α-cyclodextrin torus. The latter is fixed in the rotaxane state by a cleavable adamantane stopper at the terminal end of the ethylene glycol thread. If the stopper is connected through an ester bond, it will

be cleaved upon exposure to porcine liver esterase. Once the terminal stopper is dissociated, the torus of the rotaxane is free to be liberated, the pores can be opened and the dye can be released. The versatility of the approach and the promise it holds for sensing is evident from a look at an analogous system that has been realized a year later. Here, $Ru(bpy)_3^{2+}$ (bpy = bipyridine) has been employed as the entrapped fluorescent indicator, lactose molecules have been used instead of the rotaxane as the caps and β-D-galactosidase as the uncapping enzyme [89].

A true sensing system for the detection of methylmercury has been designed in a similar fashion as follows [90]. Again, a mesoporous silica material with a homogeneous pore size distribution (2–3 nm) and large specific surface area ($>1{,}000\ m^2g^{-1}$) is used as the scaffold. This host is loaded with a large amount of the indicator dye safranine O by simple entrapment. The pores of the hybrid material are then coated with thiol groups and closed through a reaction with squaraine dyes which are sensitive to nucleophilic attack by the thiol groups, forming 2,4-bis(4-dialkylaminophenyl)-3-hydroxy-4-alkylsulfanylcyclobut-2-enone (APC) derivatives as pore blockers. This reaction converts the deep-blue coloured squaraine into its UV-absorbing leuko form (Fig. 14) [91]. Besides closing the pores, the sulfanyl-blocked APC leuko form of the squaraine is sensitive to thiophilic ionic mercury species, attack of which leads to a cleavage of the thiol–squaraine bond and restoration of the highly fluorescent squaraine fluorophore [92]. Since the aim of this study has been to target selectively methylmercury, an extraction step has been included in the protocol to discriminate against inorganic mercury species. In the final detection reaction, the presence of CH_3Hg^+ leads to the release of the squaraine dye, which entails the release of ca. 200 safranine O molecules per squaraine molecule from the uncapped pores [90]. Besides dramatic signal amplification, a unique feature of this system is that liberation of the safranine O molecules and restoration of the squaraine dyes, both absorbing and emitting in a different wavelength range, can be used for ratiometric signal assessment, a very useful aspect for self-calibrated analytical protocols.

Mechanistically, the gating reaction of this system involves the chemodosimetric production of a fluorophore. “Chemodosimetric” here means that the reaction of an analyte with a dye molecule precursor (or leuko dye) yields a fluorescent dye molecule and that these reaction events can be counted in a fashion that is similar to counting statistics in radiation measurements. An additional gain in signal enhancement is immanent to this increasingly popular technique: a non-fluorescent precursor, and thus a virtually zero-background, is converted into a fluorophore, the PLQY of which then determines the sensitivity of this reaction. Although this chemodosimetric approach gained rapidly in popularity for molecular indicators during the last decade [93], its implementation with nanoparticulate sensing systems has only been realized in a few examples so far. The reason for the latter is perhaps related to the fact that the reaction-based detection usually relies on a very selective reaction and thus does not require a supramolecularly

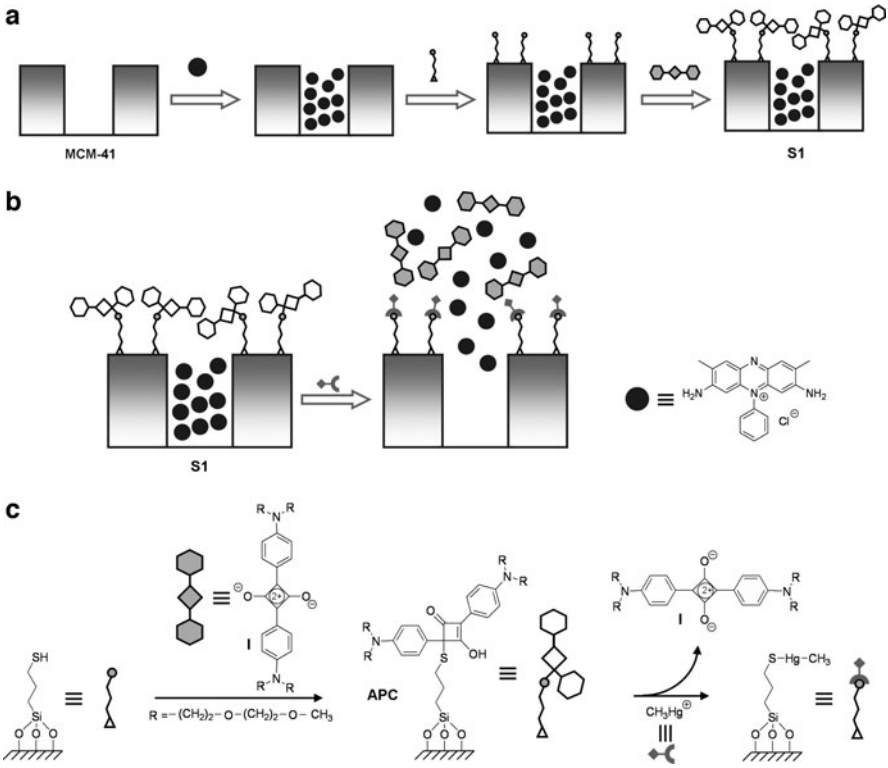

Fig. 14 (**a**) Synthetic scheme for the preparation of the safranine-entrapped and APC-capped material, (**b**) sensing mechanism and (**c**) molecular basis of the synthesis and sensing reaction. (Reprinted with permission from [90]. Copyright 2009 Wiley-VCH)

enhanced specificity. However, as the example above has shown, true massive signal amplification can arise from adequately designed systems.

4 Nanoparticles as Catalysts and Activity Enhancers

Chemical reactions in combination with nanoparticles can not only be used to unblock a large number of confined dyes and thus trigger the release of many more signalling units per binding event – they can also be used in a catalytic manner to produce directly light in a chemiluminescence (CL) reaction. CL detection in combination with particles has been realized in various ways. Whereas most of these approaches rely on a particle-based extraction step with subsequent CL detection, i.e. on a protocol in which no direct particle-mediated amplification

step is involved, only few strategies directly utilize nanoparticles in a catalytic fashion. Herein, we will focus on the latter cases; for a recent discussion of the others examples the reader is referred to [94].

4.1 Gold Nanoparticles as Catalysts in Chemiluminescence Reactions

Until today, systems that utilize metal nanoparticles as the catalysts in chemiluminescence reactions have been investigated mainly from a fundamental research point of view, most often employing gold nanoparticles (AuNPs) as the catalytic element [95–98]. AuNPs are known for their strongly size-dependent properties such as redox and photodynamic activity [24, 25]. For chemiluminescence systems involving luminol as the chemiluminescent reactant, various examples with different oxidants have been investigated and revealed a remarkable dependence on the particle size of AuNPs. If hydrogen peroxide is used as the oxidant, AuNPs with a diameter of 38 nm yield the highest chemiluminescence intensity [98]. In contrast, for ferrocyanide $[Fe(CN)_6]^{3-}$ 25-nm AuNPs show optimum performance [96]. Mechanistically, the oxidation of luminol is catalyzed in these cases by AuNPs as shown in Fig. 15.

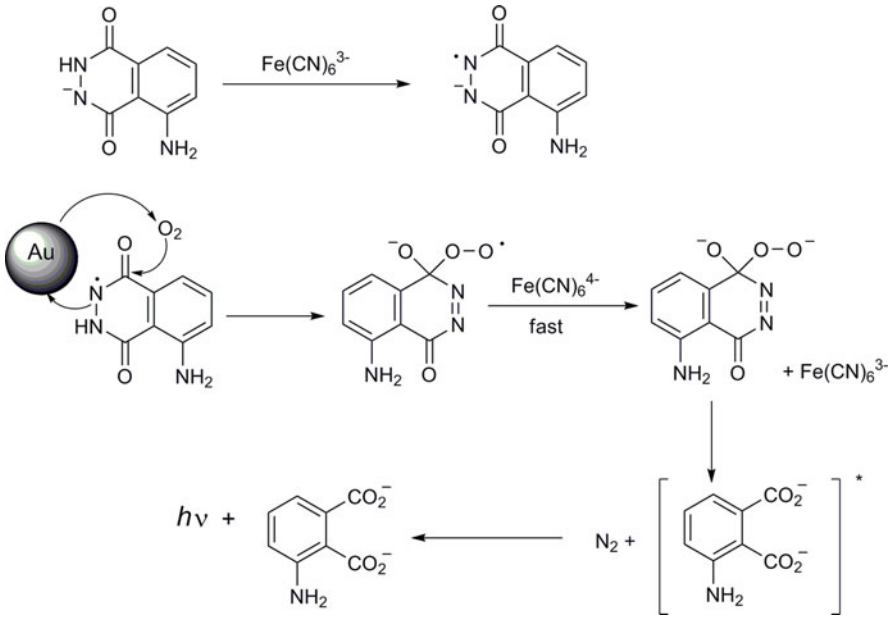

Fig. 15 AuNP-catalyzed oxidation of luminol with ferrocyanide (the AuNP-catalyzed step is more or less the same in the other systems mentioned). (Adapted from [96])

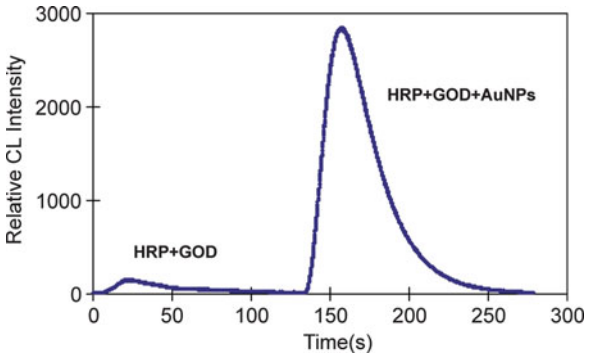

Fig. 16 Amplification effect of AuNPs on the HRP/GOD/luminol-based glucose detection. (Reprinted with permission from [100]. Copyright 2008 Elsevier)

In a recent example, Safavi et al. have shown that smaller AuNPs of 15 nm diameter yield the highest CL intensity in a AuNP-catalyzed luminol-hydrazine system. Here, the AuNPs play a double role as they first catalyze the formation of hydrogen peroxide and nitrogen from hydrazine and dissolved oxygen and secondly the subsequent oxidation of luminol by hydrogen peroxide [97].

4.2 Gold Nanoparticles as Activity Enhancers of Enzymes

It is well-known that gold nanoparticles can provide a suitable environment for redox active proteins to retain an activity like in their native environment [99]. Thus, the incorporation of AuNPs in enzyme-based chemiluminescence sensing systems is an obvious strategy and first examples have been recently published. For instance, Lan et al. could show that AuNPs greatly enhance the activity of a flow sensor for glucose based on glucose oxidase (GOD) and horseradish peroxidase (HRP) when the enzymes are co-immobilized on the gold particles via a sol-gel process [100]. The detection is based on the oxidation of glucose to D-gluconic acid and hydrogen peroxide by GOD and subsequent reaction of the peroxide with luminol under HRP-mediated catalysis, producing the well-known 2-amino-phthalic acid in its excited state (see Fig. 15). As Fig. 16 illustrates, the electron withdrawing effect of the gold nanoparticles amplifies the reaction about 20 times. Because the optimum size of the AuNPs for this reaction is 8 nm, it is unlikely that the AuNPs directly catalyze the oxidation of luminol with hydrogen peroxide; as mentioned above, the optimum size for this direct catalytic involvement has been determined to 38 nm.

4.3 Particle-Mediated Enhancement of Electrochemiluminescence

Because electrochemiluminscence (or electrogenerated chemiluminescence, ECL) is a valuable detection technique in analytical and especially bioanalytical chemistry [101], it is not surprising that nanoparticles have also been applied as enhancers in this context. Again, as for CL, the catalytic effect of AuNPs is also exploited in ECL applications. For instance, generation of ECL by luminol in an alkaline aqueous solution could be dramatically increased by up to three orders of magnitude when using a nanoparticle self-assembled electrode instead of a bulk electrode [102]. In this case, not only is the ECL signal directly assigned to the oxidation of luminol amplified, but the authors have found a new ECL signal at more negative potentials (vs SCE) which is not visible with the bulk electrode, indicating that AuNPs are necessary for the generation of this signal. The nanoparticle self-assembled electrode has also been shown to be stable for at least 1 month when stored in deionized water, even if it has been applied to cyclovoltammetric scans ranging from 1.52 to −1.49 V (vs SCE).

In a different approach not relying on AuNP–luminol redox chemistry, it has been shown that the incorporation of the well-known ECL-active dye $Ru(bpy)_3^{2+}$ into silica nanoparticles can increase the ECL intensity about three orders of magnitude compared to the free dye by limiting self-quenching phenomena [103]. However, the mechanism of ECL in silica particles is rather complex and presumably depends on parameters such as the concentration and diffusion properties of a co-reactant (e.g. tripropylamine). For instance, the co-reactant is crucial to activate ECL if the $Ru(bpy)_3^{2+}$-containing core is completely passivated by the silica shell and resistant to direct oxidation or reduction, i.e. if the distance from the electrode is too large [104].

5 Plasmonic Strategies to Luminescence Amplification

Besides chemical amplification concepts and the quest for ultimately reducing background and autofluorescence signals or increasing the number of fluorophores that are affected by the binding event, a physical strategy to pronounced modulation of luminescence signals involving particles has received increasing attention in recent years, i.e. enhancement through coupling of luminescence with SPR phenomena [105, 106]. After early theoretical treatments [107, 108] and first experimental verifications [109, 110] of the changes in the fluorescence behaviour of dye molecules in closer vicinity to metal surfaces, especially Lakowicz and co-workers have developed a new technique they called radiative decay engineering (RDE) and have utilized it in the context relevant within this article [111]. In contrast to the classic strategy of tuning fluorescent indicator molecules toward “light-up”

applications, i.e. to install an efficient quenching (or RET) process which is revived (altered) after target binding and thus to modulate the non-radiative decay rate [10], RDE basically operates with a change of the radiative decay rate. This effect results in (often) dramatically reduced fluorescence lifetimes and increased radiative rate constants which both lead to a (greatly) enhanced fluorescence quantum yield of the fluorophore [112]. This unusual increase in PLQY is supposed to originate from the enhancement of the local electromagnetic field near the metal particles under SPR conditions. Today, the main analytical applications of RDE lie in the fields of DNA hybridization and immunoassay research.

5.1 Surface Plasmon Resonance and Fluorescence

Before discussing the implications of a metal particle environment on a chromophore or a RET pair in the context of sensing, a brief introduction to SPR and fluorescence is necessary. Surface plasmons can be considered as propagating electron density waves, i.e. collective charge-density oscillations, occurring at the interface between two materials, commonly a metal and a dielectric. If excited at a certain angle of incidence by an electromagnetic wave, electromagnetic coupling between the interfaces can occur and give rise to SPR [112]. When a dye molecule is present at an adequate distance from this plasmon source it can experience a strong enhancement of its fluorescence output as sketched in the following [113].

5.1.1 Fluorescence Enhancement at a Metal Surface

Amplified fluorescence near a metal surface depends first of all on the strength of the local electromagnetic field in close vicinity to the surface and is usually quantified for a fluorophore near a metal surface relative to the same fluorophore near an inert, metal-free surface under identical illumination conditions by the so-called apparent quantum yield Y according to (4) [114, 115].

$$Y = |L(\omega_{\mathrm{exc}})|^2 Z(\omega_{\mathrm{em}}) \text{ with } \quad Z(\omega_{\mathrm{em}}) = \frac{\Phi^{\mathrm{M}}}{\Phi^{0}}. \tag{4}$$

Here, $L(\omega_{\mathrm{exc}})$ corresponds to the excitation intensity acting on the fluorophore. This quantity is enhanced by the presence of a local field, for instance, as a consequence of particle surface plasmon excitation. The possible enhancement features are determined by object and surface properties such as the particle size and shape or the roughness of a surface layer and the nature of the metallic material. For example, Kümmerlen et al. have reported that a sizeable enhancement of the local field of ca. 140 times can be found for spheroids or rods (of ca. 3:1 aspect ratio) at the tips of these objects [116]. Since the intensity is proportional to the

squared field strength, these effects can result in a 10^4-fold or larger increase in the rate of excitation.

In (4), $Z(\omega_{em})$ is the relative radiation yield and corresponds to the PLQY of a dye in the presence of metal particles Φ^M relative to its unperturbed or intrinsic PLQY Φ^0. Without going too far into theoretical details (see, e.g. [116]), two cases of fluorophores can be distinguished. For a fluorophore with a high intrinsic Φ^0, the achievable enhancement is weak. However, for a dye with a low Φ^0, high enhancement (with a limiting $Z(\omega_{em})$ factor of $[\Phi^0]^{-1}$) can result when the fluorophore can efficiently couple with the metal and the latter can act as an antenna to radiate a photon before the excitation is dissipated by non-radiative pathways within the dye molecule, corresponding to an enhancement of the radiative rate.

However, in contrast to surface enhanced Raman scattering (SERS), maximal enhancement of fluorescence is not observed from molecules that are directly adsorbed on the surface, but from those that are located at a short distance away from the metal surface. The reasons are two counterbalancing effects and can be deduced from Fig. 17a [117]. First, if positioned too close to the metal surface, Förster-type energy transfer can set in and $Z(\omega_{em})$ is rapidly reduced because of the onset of non-radiative quenching (Fig. 17a, dotted line; for the influence on the radiative rate constant, see Sect. 2.1) [118]. Second, if the dye is placed too far from the metal surface, coupling is inefficient because the induced field is an evanescent field and its intensity decays exponentially with the distance from the surface (Fig. 17a, solid line). For instance, considering a gold surface and water as the dielectric, the field has decayed to 1/e at ca. 150 nm. Thus, a maximum enhancement $Z(\omega_{em})$ exists only in a small zone at an optimum distance from the metal surface. For the Au/water system in

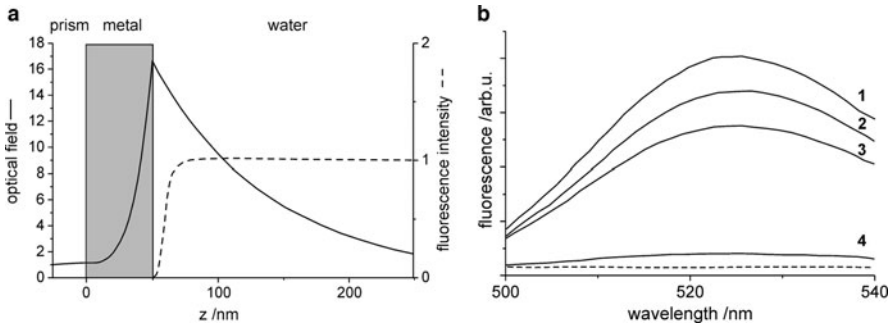

Fig. 17 (**a**) Schematic comparison of the distance dependence of the optical field of a surface plasmon mode, resonantly excited at a prism/50 nm Au/water interface (*solid line*) and the distance-dependent energy transfer-type quenching mechanism above the metal/water interface expressed as the relative fluorescence intensity (*dashed line*). (**b**) Emission spectra of biotin-FITC conjugates bound to the top avidin layer of six (1), four (2) and two (3) monolayers of an alternating BSA-biotin/avidin layer-by-layer (LbL) assembly on the surface of non-aggregated colloidal metal films. Trace (4) shows the characteristic emission spectrum obtained from a multi-LbL assembly adsorbed on bare glass slides (*dashed line*: background). (Adapted with permission from [113, 118]. Copyright 2000 Elsevier and 1998 American Chemical Society)

Fig. 17a, the surface electromagnetic field can be ca. 17 times as high as that in free space and the fluorescence intensity can be enhanced up to eightfold [119]. With regard to silver as the other metal substrate that plays a major role in SPR-based fluorescence applications and a bovine serum albumin-(BSA-) biotin/avidin multilayer system for distance adjustment, Cotton and co-workers could show that a monolayer yields only an 8-fold enhancement of the fluorescence while 6 layers increased the intensity gain to 15-fold (Fig. 17b) [118].

5.1.2 Radiative Decay Engineering

Taking a closer look at the photophysical processes that are active in an excited fluorophore, the concept of RDE becomes evident. The two parameters that are important here are the PLQY Φ and lifetime τ. The latter is a measure for the average time a fluorophore spends in the excited state before returning to the ground state by emitting a photon. It is an important criterion for the photostability of a fluorophore because photo-decomposition occurs during the lifetime of the excited state, i.e. a short lifetime or high decay rate commonly guarantees a low photobleaching rate.

In an inert environment, Φ^0 and τ^0 of a fluorophore are determined by the radiative (Γ) and non-radiative (k_{nr}) decay rates according to (5) and (6).

$$\Phi^0 = \frac{\Gamma}{\Gamma + k_{nr}}. \tag{5}$$

$$\tau^0 = (\Gamma + k_{nr})^{-1}. \tag{6}$$

Because Γ depends on the oscillator strength of an electronic transition and is largely independent of the dye's environment, for the classical case of a fluorophore as mentioned above in the introduction of Sect. 5, the only way to increase Φ^0 is to reduce k_{nr}. According to (6), however, this will also entail an increase in τ^0. A gain in both intensity and photostability thus cannot be achieved at the same time by the conventional strategy.

The RDE concept of placing the fluorophore in the presence of a metal surface (either metal nanoparticles or a thin, roughened metal layer) now takes advantage of the fact that the interaction can be described by the introduction of a new decay path Γ^M. PLQY and lifetime are then given by (7) and (8). As Γ^M increases, Φ^M increases but τ^M decreases, i.e. both PLQY and photostability are gained. The RDE concept is often also referred to as the concept of metal-enhanced fluorescence (MEF).

$$\Phi^M = \frac{\Gamma + \Gamma^M}{\Gamma + \Gamma^M + k_{nr}}. \tag{7}$$

$$\tau^M = \left(\Gamma + \Gamma^M + k_{nr}\right)^{-1}. \tag{8}$$

5.2 MEF-Based Signalling Applications

In an exemplary work, Lakowicz and co-workers have used the MEF strategy to increase the detectability of Cy3- and Cy5-labeled DNA on solid substrates covered with silver island films (SIFs) and have found a five- to tenfold increase in intensity from the silver particle-coated quartz substrate compared with uncoated quartz (Fig. 18) [120]. As one would expect from the aforementioned, these enhanced intensities have been accompanied by dramatically shortened fluorescence lifetimes, which in turn has led to a significantly higher photostability of Cy3 and Cy5 in the presence of the silver nanoparticles (AgNPs). In this study, the SIFs have been composed of silver nanoparticles with a diameter of 100–300 nm.

From the point of view of label-free luminescence detection, the MEF concept also harbours a certain potential. If small silver nanoparticles are produced in the SIF deposition process for which the surface plasmon absorption band is close to the short wavelength limit (ca. 420 nm; the practical limit in solution for AgNPs of ca. 10 nm diameter is ~400 nm [121]), direct amplification of the native DNA fluorescence is possible (Fig. 19) [122]. In this study, a remarkable 80-fold intensity enhancement has been observed. However, the authors have pointed out that only 1/25th of the DNA molecules dissolved in solution resides in the active MEF region, potentially making it possible to increase the enhancement to >1,000 when the localization of the target with respect to the SIF is better controlled. Again, as shown in Fig. 19, the increase in intensity is accompanied by a reduction of the fluorescence lifetime. Such strong amplification would render this method very interesting for DNA sequencing applications without extrinsic labelling.

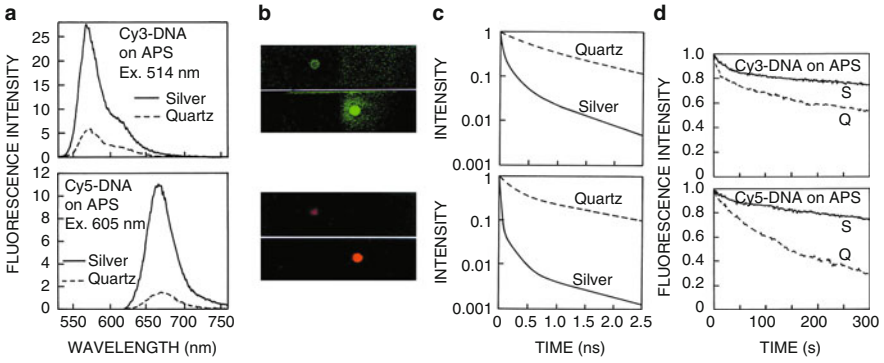

Fig. 18 (**a**) Emission spectra, (**b**) photographs and (**c**) fluorescence decays of the labelled DNA oligomers on neat quartz and SIF-coated quartz substrates. The quartz was treated with aminopropyltriethoxysilane (APS). (**d**) Photostability of Cy3-DNA and Cy5-DNA on APS-treated slides with and without SIFs. The excitation intensity was adjusted to yield the same emission intensities on neat and SIF-quartz. (Reprinted with permission from [120]. Copyright 2003 BioTechniques)

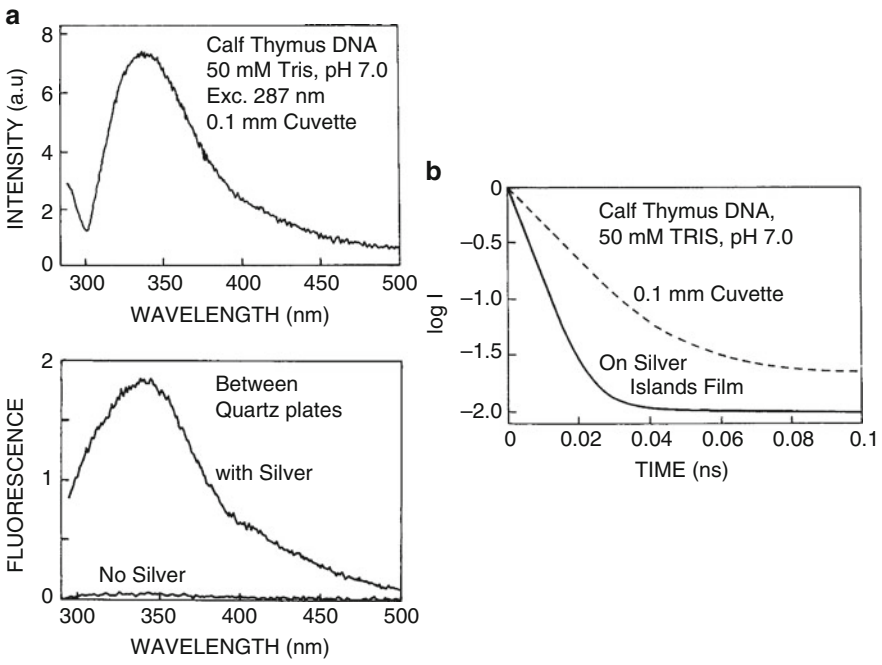

Fig. 19 (**a**) Emission spectrum of a buffered solution containing calf thymus DNA in a cuvette (*top*) and between quartz plates in the absence (labelled "No Silver") and the presence of a SIF (labelled "with Silver"; *bottom*). (**b**) Decay of the fluorescence of calf thymus DNA in the absence (*dashed line*) and presence of a SIF (*solid line*). (Reprinted with permission from [122]. Copyright 2001 Academic Press/Elsevier)

5.2.1 MEF and Multiphoton Excitation

Two-photon or multi-photon excitation is a nonlinear absorption process in which fluorophores are excited with several photons of low energy. This technique offers the possibility to excite a fluorophore with rather long wavelengths, often in the NIR spectral region, which is especially attractive in bioimaging applications [123]; see also Sect. 2.3. At long wavelengths, scattering is significantly reduced, penetration of tissue enhanced and autofluorescence commonly negligible. However, the excitation rate is highly dependent on the excitation intensity and proportional to its square, i.e. usually comparatively strong laser excitation is required. Nonetheless, the employment of metal nanoparticles for which the above-mentioned field enhancement is operative can also lead to strong enhancement factors for multi-photon excitation processes of up to 10^8 [124].

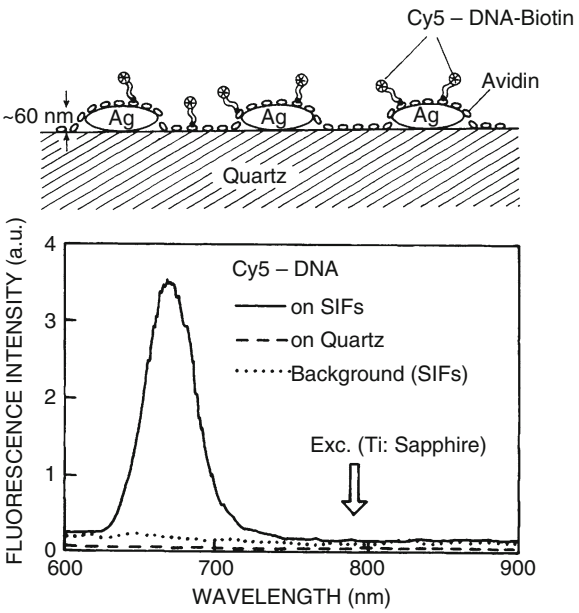

Fig. 20 Two-photon-excited emission spectra of Cy5-DNA on neat and SIF-coated quartz. The brightness of Cy5-DNA on SIFs is approximately 100-fold higher than on quartz. The *top panel* shows a sketch of the Cy5 deposited on SIFs. (Reprinted with permission from [125]. Copyright 2005 Academic Press/Elsevier)

As shown in Fig. 20, Lukomska et al. could realize a ca. 100-times amplified fluorescence signal with Cy5 by using a Ti-Sapphire laser and NIR excitation [125]. The authors have found that the average fluorescence lifetimes $<\tau>$ of Cy5 on the SIF substrates are considerably reduced compared with the dye on a neat quartz support. In addition, they could show that $<\tau>$ for one- and two-photon excitation were rather similar, $<\tau> = 0.108$ and 0.117 ns, respectively, indicating that the intensity enhancement is mainly due to a stronger local field near the metal surface.

5.2.2 Metal Enhanced Phosphorescence

Besides fluorescence, another radiative decay path of an excited molecule is phosphorescence, which occurs from the lowest triplet state T_1 to the ground state S_0. Such intersystem crossing is a highly forbidden process and therefore phosphorescence decay is significantly slower compared with fluorescence, commonly in the micro- to millisecond time regime. As mentioned above for the rare earth emitters as RET donors in Sect. 2, long lifetimes harbour the advantage of sensitive detection by time-resolved or time-gated spectroscopic methods. Provided that

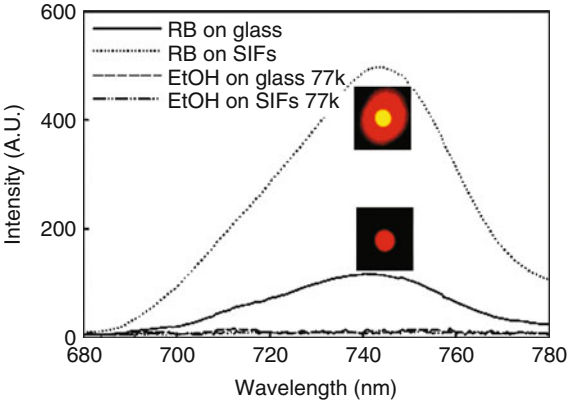

Fig. 21 Phosphorescence spectra of Rose Bengal immobilized on an organic glass with and without SIFs at 77 K (λ_{exc} = 532 nm). (Reprinted with permission from [129]. Copyright 2006 American Chemical Society)

adequate probes are available, these features can also yield valuable information on rotational motions of proteins or particles on the micro- to millisecond time-scale through time-resolved phosphorescence anisotropy measurements [126–128].

To enhance the often weak phosphorescence signals, SPR-based coupling techniques can also be employed. For instance, Zhang et al. have reported a five times amplified phosphorescence emission for the dye Rose Bengal close to a SIF-covered glass surface compared with neat glass (Fig. 21) [129]. Detailed investigations as a function of temperature have revealed that the phosphorescence enhancement factor is temperature-dependent, increasing from 3.2 at room temperature to 5.7 at 77 K. The authors could further detect both, MEP and MEF, and explained this coexistence by enhanced absorption and reverse intersystem crossing involving a $S_1 \leftarrow T_1$ path.

5.2.3 Metal Nanoparticle-Enhanced RET

In the 1980s, first theoretical works have been published which described how the vicinity of metal particles could increase the RET efficiency in donor–acceptor systems [130, 131]. Instead of increased rates of radiative decay as found for fluorophores close to a metal surface, see above, the effect here is based on increased rates of resonance energy transfer. This enhancement of the RET rate has been predicted to increase by 100-fold at distances up to 700 Å, i.e. covering distances that are ca. tenfold larger than the Förster distances commonly achieved in bulk solution. Early studies on the calf thymus model DNA system (see Fig. 19) employing the minor groove-binding dye DAPI (4′,6-diamidino-2-phenylindole) and the intercalating dye propidium iodide (PI) in the presence of SIFs have shown that the effective interaction distance R_0 of such non-covalently interacting systems can be increased fivefold [132]. For instance, for covalently labelled model systems FRET rates can increase by >20-fold for the Cy5/Cy5.5 pair conjugated to complementary oligonucleotides [133]. In a subsequent study employing silver particles

of 15, 40 and 80 nm diameter and varying the distances between the FRET dye pair and the particle surface (and not the distance between D_{RET} and A_{RET}), it has been found that the amplification of FRET increases with increasing nanoparticle size and that FRET is more efficient if the D_{RET}/A_{RET} pair is located 10 nm above the surface instead of 2 nm [134].

Another interesting example of using modified AgNPs instead of SIFs to detect donor–acceptor proximity over a longer distance than the standard Förster range has been published recently. Lessard-Viger et al. have employed novel multilayer core-shell nanoparticles featuring a silver core surrounded by silica layers containing FRET donor and acceptor positioned at a precise distance from the core [135]. The presence of silver results in an increase in Förster efficiency by a factor of 4 and an increase in Förster range of ~30%.

Finally, we conclude this section with first approaches toward plasmonically enhanced RET systems using QDs. In 2007, Govorov et al. have investigated theoretically the possibilities of how RET between pairs of CdTe QDs, InGaN QDs and PbSe QDs can be enhanced by the presence of AgNPs and AuNPs [136]. A year later, Komarala et al. have experimentally investigated CdTe QD RET pairs, i.e. CdTe QDs of different size acting as D_{RET} and A_{RET}, and the enhancement of the energy transfer processes by AuNPs [137]. In contrast to the QD luminophore–AuNP quencher-type RET systems introduced in Sect. 2.2, the present approach shows true aspects of amplification yet requires more careful control.

In conclusion, all the examples discussed in this section require more attention with respect to architectural control when aiming at high (amplified) performance. At the same time, the nanoparticle chemistry used in most of these cases is quite simple, basically due to the physical nature of the processes responsible for amplification and a great variety of conventional chromophore systems can be employed in these MEF-based applications.

6 Conclusion

The present contribution has shown how versatile and manifold the application of luminescent nano- and microparticles in analytical and bioanalytical contexts that rely on signal amplification strategies is already today. The different applications range from utilizing mainly the particles' size, by doping particles with a large amount of emitters or by storing a large number of emitters in a porous particle network, over the catalytic (chemical) properties of NPs and physical enhancement effects to particular physical properties such as multi-photon excitation. The nature of the particles itself has been rather diverse and their combination with organic or bioorganic entities is almost limitless. The examples presented here have shown that today, amplification factors of more than three orders of magnitude can be readily accomplished.

In the last 10–15 years of research which showed the utmost activity in the field, so many different approaches have been realized that it is difficult to say where the

journey will lead to next. One approach that we believe will receive increasing interest is the combination of gold nanoparticles with QDs in applications where the AuNPs do not act as simple quenchers, but where the AuNPs amplify the luminescence of their semiconductor twins. First approaches have been realized recently, for instance, with CdSe QDs [138]. Alternatively, luminescence enhancement in 3D arrays of QDs in lamellar objects of micrometric size is possible by integrating small AuNPs [139]. Since these lamellae are also permeable for small molecules or ions, such structures are potentially suitable as sensory (micro)membranes.

With respect to efficiency and amplification, nature has created some of the best performing ensembles. Gated systems relying on the liberation of many indicators from a reservoir once the gate is unlocked resemble gated membrane channels in natural systems. Their development is also only at the beginning so far. For instance, if such gated systems are not only loaded with many indicators but are also equipped with a catalytic indication system on the outside, the arrival of one analyte can trigger the formation of many "catalytic keys", unlocking many of the gates and liberating a very large number of the doped cargo. Truly massive amplification might thus arise. In the field of improving the optical properties of photosynthetic systems, a combination of coupling with QDs and invoking RET processes has already achieved promising results [140]. With respect to RET and metal nanoparticle-based enhancement, the introduction of electrochemiluminescent systems besides BRET and CRET offers another degree of flexibility and performance for "dark" excitation and first QD-based approaches have been realized lately [141].

Finally, when talking about amplifying nanoparticles, the applications are of course not only limited to spherical particles as mainly employed today and discussed here, but aspherical objects like cages, rods or wires offer a wealth of additional tuning modes and will presumably receive pronounced attention in the future [142].

References

1. Lakowicz JR (ed) (1992–2006) Topics in fluorescence spectroscopy series, vols 1–11. Plenum, New York and Springer, Berlin
2. Wolfbeis OS (ed) (2001–2008) Springer series on fluorescence, vols 1–6. Springer, Berlin
3. Demchenko A (2009) Introduction to fluorescence sensing. Springer, Berlin
4. Seidel M, Gauglitz G (2003) Miniaturization and parallelization of fluorescence immunoassays in nanotiter plates. Trends Anal Chem 22:385–394
5. LaFratta CN, Walt DR (2008) Very high density sensing arrays. Chem Rev 108:614–637
6. Hunt HC, Wilkinson JS (2008) Optofluidic integration for microanalysis. Microfluid Nanofluid 4:53–79
7. Myers FB, Lee LP (2008) Innovations in optical microfluidic technologies for point-of-care diagnostics. Lab Chip 8:2015–2031
8. Rurack K, Resch-Genger U (2002) Rigidization, preorientation and electronic decoupling – the 'magic triangle' for the design of highly efficient fluorescent sensors and switches. Chem Soc Rev 31:116–127

9. Gill P, Ghaemi A (2008) Nucleic acid isothermal amplification technologies – a review. Nucleosides Nucleotides Nucleic Acids 27:224–243
10. Descalzo AB, Zhu S, Fischer T et al (2010) Optimization of the coupling of target recognition and signal generation. In: Demchenko AP (ed) Advanced fluorescence reporters in chemistry and biology. II. Molecular constructions, polymers and nanoparticles. Springer, Berlin, pp 41–106
11. Roda A, Guardigli M, Michelini E et al (2009) Nanobioanalytical luminescence: Förster-type energy transfer methods. Anal Bioanal Chem 393:109–123
12. Sapsford KE, Berti L, Medintz IL (2006) Materials for fluorescence resonance energy transfer analysis: beyond traditional donor–acceptor combinations. Angew Chem Int Ed 45:4562–4588
13. Förster T (1948) Intermolecular energy migration and fluorescence. Ann Phys 2:55–75
14. Braslavsky SE (2007) Glossary of terms used in photochemistry. 3rd edition (IUPAC Recommendations 2006). Pure Appl Chem 79:293–465
15. Boute N, Jockers R, Issad T (2002) The use of resonance energy transfer in high-throughput screening: BRET versus FRET. Trends Pharmacol Sci 23:351–354
16. Eidne KA, Kroeger KM, Hanyaloglu AC (2002) Applications of novel resonance energy transfer techniques to study dynamic hormone receptor interactions in living cells. Trends Endocrinol Metab 13:415–421
17. Chen J, Zeng F, Wu S et al (2009) A facile approach for cupric ion detection in aqueous media using polyethyleneimine/PMMA core-shell fluorescent nanoparticles. Nanotechnology 20:365502
18. Roberts DV, Wittmershaus BP, Zhang YZ et al (1998) Efficient excitation energy transfer among multiple dyes in polystyrene microspheres. J Lumin 79:225–231
19. Weissleder R (2001) A clearer vision for in vivo imaging. Nat Biotechnol 19:316–317
20. Wang L, Tan W (2006) Multicolor FRET silica nanoparticles by single wavelength excitation. Nano Lett 6:84–88
21. Chen X, Estevez MC, Zhu Z et al (2009) Using aptamer-conjugated fluorescence resonance energy transfer nanoparticles for multiplexed cancer cell monitoring. Anal Chem 81:7009–7014
22. Bünzli JCG, Piguet C (2005) Taking advantage of luminescent lanthanide ions. Chem Soc Rev 34:1048–1077
23. Härmä H, Soukka T, Lövgren T (2001) Europium nanoparticles and time-resolved fluorescence for ultrasensitive detection of prostate-specific antigen. Clin Chem 47:561–568
24. Daniel MC, Astruc D (2004) Gold nanoparticles: assembly, supramolecular chemistry, quantum-size-related properties, and applications toward biology, catalysis, and nanotechnology. Chem Rev 104:293–346
25. Wei Q, Wei A (2010) Signal generation with gold nanoparticles: photophysical properties for sensor and imaging applications. In: Rurack K, Martínez-Máñez R (eds) The supramolecular chemistry of organic-inorganic hybrid materials. Wiley, Hoboken, NJ, pp 319–349
26. Dulkeith E, Ringler M, Klar TA et al (2005) Gold nanoparticles quench fluorescence by phase induced radiative rate suppression. Nano Lett 5:585–589
27. Huang CC, Chang HT (2006) Selective gold-nanoparticle-based "turn-on" fluorescent sensors for detection of mercury(II) in aqueous solution. Anal Chem 78:8332–8338
28. He X, Liu H, Li Y et al (2005) Gold nanoparticle-based fluorometric and colorimetric sensing of copper(II) ions. Adv Mater 17:2811–2815
29. Mayilo S, Kloster MA, Wunderlich M et al (2009) Long-range fluorescence quenching by gold nanoparticles in a sandwich immunoassay for cardiac tropnini T. Nano Lett 9: 4558–4563
30. Ray PC, Fortner A, Darbha GK (2006) Gold nanoparticle based FRET assay for the detection of DNA cleavage. J Phys Chem B 110:20745–20748
31. Gill R, Zayats M, Willner I (2008) Semiconductor quantum dots for bioanalysis. Angew Chem Int Ed 47:7602–7625

32. Frasco MF, Chaniotakis N (2010) Bioconjugated quantum dots as fluorescent probes for bioanalytical applications. Anal Bioanal Chem 396:229–240
33. Jorge PAS, Martins MA, Trindade T et al (2007) Optical fiber sensing using quantum dots. Sensors 7:3489–3534
34. Han M, Gao X, Su JZ et al (2001) Quantum-dot-tagged microbeads for multiplexed optical coding of biomolecules. Nat Biotechnol 19:631–635
35. Clapp AR, Medintz IL, Mattoussi H (2006) Förster resonance energy transfer investigations using quantum-dot fluorophores. ChemPhysChem 7:47–57
36. Algar WR, Krull UJ (2008) Quantum dots as donors in fluorescence resonance energy transfer for the bioanalysis of nucleic acids, proteins, and other biological molecules. Anal Bioanal Chem 391:1609–1618
37. Lee S, Park K, Kim K et al (2008) Activatable imaging probes with amplified fluorescent signals. Chem Commun 4250–4260
38. Hering VR, Gibson G, Schumacher RI et al (2007) Energy transfer between CdSe/ZnS core/shell quantum dots and fluorescent proteins. Bioconjug Chem 18:1705–1708
39. Willard DM, Mutschler T, Yu M et al (2006) Directing energy flow through quantum dots: towards nanoscale sensing. Anal Bioanal Chem 384:564–571
40. Tomczak N, Janczewski D, Han MY et al (2009) Designer polymer-quantum dot architectures. Prog Polym Sci 34:393–430
41. Freeman R, Li Y, Tel-Vered R et al (2009) Self-assembly of supramolecular aptamer structures for optical or electrochemical sensing. Analyst 134:653–656
42. Goldman ER, Medintz IL, Whitley JL et al (2005) A hybrid quantum dot-antibody fragment fluorescence resonance energy transfer-based TNT sensor. J Am Chem Soc 127:6744–6751
43. Wang X, Guo X (2009) Ultrasensitive Pb^{2+} detection based on fluorescence resonance energy transfer (FRET) between quantum dots and gold nanoparticles. Analyst 134:1348–1354
44. Tang B, Cao L, Xu K et al (2008) A new nanobiosensor for glucose with high sensitivity and selectivity in serum based on fluorescence resonance energy transfer (FRET) between CdTe quantum dots and Au nanoparticles. Chem Eur J 14:3637–3644
45. Jiang G, Susha AS, Lutich AA et al (2009) Cascaded FRET in conjugated polymer/quantum dot/dye-labeled DNA complexes for DNA hybridization detection. ACS Nano 12:4127–4131
46. So MK, Xu C, Loening AM et al (2006) Self-illuminating quantum dot conjugates for in vivo imaging. Nat Biotechnol 24:339–343
47. Huang X, Li L, Qian H et al (2006) A resonance energy transfer between chemiluminescent donors and luminescent quantum-dots as acceptors (CRET). Angew Chem Int Ed 45:5140–5143
48. Zhao S, Huang Y, Shi M et al (2010) Chemiluminescence resonance energy transfer-based detection for microchip electrophoresis. Anal Chem 82:2036–2041
49. Naruke H, Mori T, Yamase T (2009) Luminescence properties and excitation process of a near-infrared to visible up-conversion color-tunable phosphor. Opt Mater 31:1483–1487
50. Wang X, Li YD (2007) Monodisperse nanocrystals: general synthesis, assembly, and their applications. Chem Commun 2901–2910
51. Jalil RA, Zhang Y (2008) Biocompatibility of silica coated $NaYF_4$ upconversion fluorescent nanocrystals. Biomaterials 29:4122–4128
52. Wang L, Yan R, Huo Z et al (2005) Fluorescence resonant energy transfer biosensor based on upconversion-luminescent nanoparticles. Angew Chem Int Ed 44:6054–6057
53. Kuningas K, Ukonaho T, Päkkilä H et al (2006) Upconversion fluorescence resonance energy transfer in a homogeneous immunoassay for estradiol. Anal Chem 78:4690–4696
54. Rantanen T, Päkkilä H, Jämsen L et al (2007) Tandem dye acceptor used to enhance upconversion fluorescence resonance energy transfer in homogeneous assays. Anal Chem 79:6312–6318
55. Bonacchi S, Genovese D, Juris R et al (2010) Luminescent chemosensors based on silica nanoparticles. Top Curr Chem [this volume]

56. Zhou Q, Swager TM (1995) Fluorescent chemosensors based on energy migration in conjugated polymers: the molecular wire approach to increased sensitivity. J Am Chem Soc 117:12593–12602
57. Thomas SW III, Joly GD, Swager TM (2007) Chemical sensors based on amplifying fluorescent conjugated polymers. Chem Rev 107:1339–1386
58. Baier MC, Huber J, Mecking S (2009) Fluorescent conjugated polymer nanoparticles by polymerization in miniemulsion. J Am Chem Soc 131:14267–14273
59. Wu C, Szymanski C, Cain Z et al (2007) Conjugated polymer dots for multiphoton fluorescence imaging. J Am Chem Soc 129:12904–12905
60. Wu C, Bull B, Szymanski C et al (2008) Multicolor conjugated polymer dots for biological fluorescence imaging. ACS Nano 2:2415–2423
61. Moon JH, McDaniel W, MacLean P et al (2007) Live-cell-permeable poly(*p*-phenylene ethynylene). Angew Chem Int Ed 46:8223–8225
62. Howes P, Thorogate R, Green M et al (2009) Synthesis, characterisation and intracellular imaging of PEG capped BEHP-PPV nanospheres. Chem Commun 2490–2492
63. Wosnick JH, Liao JH, Swager TM (2005) Layer-by-layer poly(phenylene ethynylene) films on silica microspheres for enhanced sensory amplification. Macromolecules 38:9287–9290
64. McQuade DT, Hegedus AH, Swager TM (2000) Signal amplification of a "turn-on" sensor: harvesting the light captured by a conjugated polymer. J Am Chem Soc 122:12389–12390
65. Liu B, Bazan GC (2004) Homogeneous fluorescence-based DNA detection with water-soluble conjugated polymers. Chem Mater 16:4467–4476
66. Wang Y, Liu B (2009) Conjugated polymer as a signal amplifier for novel silica nanoparticle-based fluoroimmunoassay. Biosens Bioelectron 24:3293–3298
67. Wang Y, Liu B (2007) Silica nanoparticle assisted DNA assays for optical signal amplification of conjugated polymer based fluorescent sensors. Chem Commun 3553–3555
68. Wang Y, Liu B (2009) Conjugated polyelectrolyte-sensitized fluorescent detection of thrombin in blood serum using aptamer-immobilized silica nanoparticles as the platform. Langmuir 25:12787–12793
69. Pu KY, Li K, Liu B (2010) Cationic oligofluorene-substituted polyhedral oligomeric silsesquioxane as light-harvesting unimolecular nanoparticle for fluorescence amplification in cellular imaging. Adv Mater 22:643–646
70. Lowe M, Spiro A, Zhang YZ et al (2004) Multiplexed, particle-based detection of DNA using flow cytometry with 3DNA dendrimers for signal amplification. Cytometry A 60A:135–144
71. Wängler C, Moldenhauer G, Saffrich R et al (2008) PAMAM structure-based multifunctional fluorescent conjugates for improved fluorescent labelling of biomacromolecules. Chem Eur J 14:8116–8130
72. Balzani V, Ceroni P, Gestermann S et al (2000) Dendrimers as fluorescent sensors with signal amplification. Chem Commun 853–854
73. Balzani V, Ceroni P, Gestermann S et al (2000) Effect of protons and metal ions on the fluorescence properties of a polylysin dendrimer containing twenty four dansyl units. J Chem Soc Dalton Trans 3765–3771
74. Vögtle F, Gestermann S, Kauffmann C et al (2000) Coordination of Co^{2+} ions in the interior of poly(propylene amine) dendrimers containing fluorescent dansyl units in the periphery. J Am Chem Soc 122:10389–10404
75. Pugh VJ, Hu QS, Zuo X et al (2001) Optically active BINOL core-based phenyleneethynylene dendrimers for the enantioselective fluorescent recognition of amino alcohols. J Org Chem 66:6136–6140
76. Xu MH, Lin J, Hu QS et al (2002) Fluorescent sensors for the enantioselective recognition of mandelic acid: signal amplification by dendritic branching. J Am Chem Soc 124:14239–14246
77. Guo M, Varnavski O, Narayanan A et al (2009) Investigations of energy migration in an organic dendrimer macromolecule for sensory signal amplification. J Phys Chem A 113:4763–4771

78. Trau D, Yang W, Seydack M et al (2002) Nanoencapsulated microcrystalline particles for superamplified biochemical assays. Anal Chem 74:5480–5486
79. Chan CP, Bruemmel Y, Seydack M et al (2004) Nanocrystal biolabels with releasable fluorophores for immunoassays. Anal Chem 76:3638–3645
80. Sin KK, Chan CPY, Pang TH et al (2006) A highly sensitive fluorescent immunoassay based on avidin-labeled nanocrystals. Anal Bioanal Chem 384:638–644
81. Chan CP, Tzang LC, Sin K et al (2007) Biofunctional organic nanocrystals for quantitative detection of pathogen deoxyribonucleic acid. Anal Chim Acta 584:7–11
82. Truneh A, Machy P, Horan PK (1987) Antibody-bearing liposomes as multicolor immunofluorescence markers for flow cytometry and imaging. J Immunol Methods 100:59–71
83. Schott H, Von Cunow D, Langhals H (1992) Labeling of liposomes with intercalating perylene fluorescent dyes. Biochim Biophys Acta 1110:151–157
84. Edwards KA, Baeumner AJ (2006) Optimization of DNA-tagged liposomes for use in microtiter plate analyses. Anal Bioanal Chem 386:1613–1623
85. Rongen HAH, Bult A, van Bennekom WP (1997) Liposomes and immunoassays. J Immunol Methods 204:105–133
86. Anraku Y, Kishimura A, Oba M et al (2010) Spontaneous formation of nanosized unilamellar polyion complex vesicles with tunable size and properties. J Am Chem Soc 132:1631–1636
87. Slowing II, Trewyn BG, Lin VSY (2010) Nanogated mesoporous silica materials. In: Rurack K, Martínez-Máñez R (eds) The supramolecular chemistry of organic-inorganic hybrid materials. Wiley, Hoboken, NJ, pp 479–502
88. Patel K, Angelos S, Dichtel WR et al (2008) Enzyme-responsive snap-top covered silica nanocontainers. J Am Chem Soc 130:2382–2383
89. Bernardos A, Aznar E, Marcos MD et al (2009) Enzyme-responsive controlled release using mesoporous silica supports capped with lactose. Angew Chem Int Ed 48:5884–5887
90. Climent E, Marcos M, Martínez-Máñez R et al (2009) The determination of methylmercury in real samples using organically capped mesoporous inorganic materials capable of signal amplification. Angew Chem Int Ed 48:8519–8522
91. Ros-Lis JV, García B, Jiménez D et al (2004) Squaraines as fluoro-chromogenic probes for thiol-containing compounds and their application to the detection of biorelevant thiols. J Am Chem Soc 126:4064–4065
92. Ros-Lis JV, Marcos MD, Martínez-Máñez R et al (2005) A regenerative chemodosimeter based on metal-induced dye formation for the highly selective and sensitive optical determination of Hg^{2+} ions. Angew Chem Int Ed 44:4405–4407
93. Cho DG, Sessler JL (2009) Modern reaction-based indicator systems. Chem Soc Rev 38:1647–1662
94. Zhao L, Sun L, Chu X (2009) Chemiluminescence immunoassay. Trends Anal Chem 28:404–415
95. Lin J, Liu M (2008) Chemiluminescence from the decomposition of peroxymonocarbonate catalyzed by gold nanoparticles. J Phys Chem B 112:7850–7855
96. Duan C, Cui H, Zhang Z et al (2007) Size-dependent inhibition and enhancement by gold nanoparticles of luminol-ferricyanide chemiluminescence. J Phys Chem C 111: 4561–4566
97. Safavi A, Absalan G, Bamdad F (2008) Effect of gold nanoparticle as a novel nanocatalyst on luminol-hydrazine chemiluminescence system and its analytical application. Anal Chim Acta 610:243–248
98. Zhang Z, Cui H, Lai C et al (2005) Gold nanoparticle-catalyzed luminol chemiluminescence and its analytical applications. Anal Chem 77:3324–3329
99. Crumbliss AL, Perine SC, Stonehuerner J et al (1992) Colloidal gold as a biocompatible immobilization matrix suitable for the fabrication of enzyme electrodes by electrodeposition. Biotechnol Bioeng 40:483–490

100. Lan D, Li B, Zhang Z (2008) Chemiluminescence flow biosensor for glucose based on gold nanoparticle-enhanced activities of glucose oxidase and horseradish peroxidase. Biosens Bioelectron 24:934–938
101. Richter MM (2004) Electrochemiluminescence (ECL). Chem Rev 104:3003–3036
102. Cui H, Xu Y, Zhang Z (2004) Multichannel electrochemiluminescence of luminol in neutral and alkaline aqueous solutions on a gold nanoparticle self-assembled electrode. Anal Chem 76:4002–4010
103. Zanarini S, Rampazzo E, Della Ciana L et al (2009) $Ru(bpy)_3$ covalently doped silica nanoparticles as multicenter tunable structures for electrochemiluminescence amplification. J Am Chem Soc 131:2260–2267
104. Li M, Chen Z, Yam VWW et al (2008) Multi functional ruthenium(II) polypyridine complex-based core-shell magnetic silica nanocomposites: magnetism, luminescence, and electrochemiluminescence. ACS Nano 2:905–912
105. Das P, Metiu H (1985) Enhancement of molecular fluorescence and photochemistry by small metal particles. J Phys Chem 89:4680–4687
106. Lakowicz JR, Ray K, Chowdhury M et al (2008) Plasmon-controlled fluorescence: a new paradigm in fluorescence spectroscopy. Analyst 133:1308–1346
107. Morawitz H, Philpott MR (1974) Coupling of an excited molecule to surface plasmons. Phys Rev B 10:4863–4868
108. Philpott MR (1975) Effect of surface plasmons on transitions in molecules. J Chem Phys 62:1812–1817
109. Weber WH, Eagen CF (1979) Energy-transfer from an excited dye molecule to the surface-plasmons of an adjacent metal. Opt Lett 4:236–238
110. Benner RE, Dornhaus R, Chang RK (1979) Angular emission profiles of dye molecules excited by surface-plasmon waves at a metal-surface. Opt Commun 30:145–149
111. Lakowicz JR (2001) Radiative decay engineering: biophysical and biomedical application. Anal Biochem 298:1–24
112. Weitz DA, Garoff S, Hanson CD et al (1982) Fluorescent lifetimes of molecules on silver-island films. Opt Lett 7:89–91
113. Liebermann T, Knoll W (2000) Surface-plasmon field-enhanced fluorescence spectroscopy. Colloids Surf 171:115–130
114. Gersten J, Nitzan A (1981) Spectroscopic properties of molecules interacting with small dielectric particles. J Chem Phys 75:1139–1152
115. Wokaun A, Lutz HP, King AP et al (1983) Energy-transfer in surface enhanced luminescence. J Chem Phys 79:509–514
116. Kümmerlen J, Leitner A, Brunner H et al (1993) Enhanced dye fluorescence over silver island films: analysis of the distance dependence. Mol Phys 80:1031–1046
117. Ford GW, Weber WH (1984) Electromagnetic-interactions of molecules with metal-surfaces. Phys Rep 113:195–287
118. Sokolov K, Chumanov G, Cotton TM (1998) Enhancement of molecular fluorescence near the surface of colloidal metal films. Anal Chem 70:3898–3905
119. Knoll W (1998) Interfaces and thin films as seen by bound electromagnetic waves. Annu Rev Phys Chem 49:569–638
120. Lakowicz JR, Malicka J, Gryczynski I (2003) Silver particles enhance emission of fluorescent DNA oligomers. Biotechniques 34:62–68
121. Mafuné F, Kohno J, Takeda Y et al (2000) Formation and size control of silver nanoparticles by laser ablation in aqueous solution. J Phys Chem B 104:9111–9117
122. Lakowicz JR, Shen B, Gryczynski Z et al (2001) Intrinsic fluorescence from DNA can be enhanced by metallic particles. Biochem Biophys Res Commun 286:875–879
123. Diaspro A (1999) Introduction to two-photon microscopy. Microsc Res Tech 47:163–164
124. Gryczynski I, Malicka J, Shen Y et al (2002) Multiphoton excitation of fluorescence near metallic particles: enhanced and localized excitation. J Phys Chem B 106:2191–2195

125. Lukomska J, Gryczynski I, Malicka J et al (2005) Two-photon induced fluorescence of Cy5-DNA in buffer solution and on silver island films. Biochem Biophys Res Commun 328:78–84
126. De Beuckeleer K, Volckaert G, Engelborghs Y (1999) Time resolved fluorescence and phosphorescence properties of the individual tryptophan residues of barnase: evidence for protein-protein interactions. Proteins 36:42–53
127. Prochniewicz E, Janson N, Thomas DD et al (2005) Cofilin increases the torsional flexibility and dynamics of actin filaments. J Mol Biol 353:990–1000
128. Lettinga MP, van Kats CM, Philipse AP (2000) Rotational diffusion of tracer spheres in packings and dispersions of colloidal spheres studied with time-resolved phosphorescence anisotropy. Langmuir 16:6166–6172
129. Zhang Y, Aslan K, Previte MJR et al (2006) Metal-enhanced phosphorescence: interpretation in terms of triplet-coupled radiating plasmons. J Phys Chem B 110:25108–25114
130. Gersten J, Nitzan A (1984) Accelerated energy transfer between molecules near a solid particle. Chem Phys Lett 104:31–37
131. Hua XM, Gersten J, Nitzan A (1985) Theory of energy transfer between molecules near solid state particles. J Chem Phys 83:3650–3659
132. Lakowicz JR, Kuśba J, Shen Y et al (2003) Effects of metallic silver particles on resonance energy transfer between fluorophores bound to DNA. J Fluoresc 13:69–77
133. Zhang J, Fu Y, Lakowicz JR (2007) Enhanced Förster resonance energy transfer (FRET) on a single metal particle. J Phys Chem C 111:50–56
134. Zhang J, Fu Y, Chowdhury MH et al (2007) Enhanced Förster resonance energy transfer on single metal particle. 2. Dependence on donor-acceptor separation distance, particle size, and distance from metal surface. J Phys Chem C 111:11784–11792
135. Lessard-Viger M, Rioux M, Rainville L et al (2009) FRET enhancement in multilayer core-shell nanoparticles. Nano Lett 9:3066–3071
136. Govorov AO, Lee J, Kotov NA (2007) Theory of plasmon-enhanced Förster energy transfer in optically excited semiconductor and metal nanoparticles. Phys Rev B 76:125308
137. Komarala VK, Bradley AL, Rakovich YP et al (2008) Surface plasmon enhanced Förster resonance energy transfer between the CdTe quantum dots. Appl Phys Lett 93:123102
138. Chan YH, Chen J, Wark SE et al (2009) Using patterned arrays of metal nanoparticles to probe plasmon enhanced luminescence of CdSe quantum dots. ACS Nano 3:1735–1744
139. Lee A, Coombs NA, Gourevich I et al (2009) Lamellar envelopes of semiconductor nanocrystals. J Am Chem Soc 131:10182–10188
140. Govorov AO (2008) Enhanced optical properties of a photosynthetic system conjugated with semiconductor nanoparticles: the role of Förster transfer. Adv Mater 20:4330–4335
141. Shan Y, Xu JJ, Chen HY (2009) Distance-dependent quenching and enhancing of electrochemiluminescence from a CdS: Mn nanocrystal film by Au nanoparticles for highly sensitive detection of DNA. Chem Commun 905–907
142. Shegai T, Huang Y, Xu H et al (2010) Coloring fluorescence emission with silver nanowires. Appl Phys Lett 96:103114